

Classification of Gapped Domain Walls of Topological Orders in 2+1 dimensions: A Levin-Wen Model Realization

Yanyan Chen^a Siyuan Wang^a Yu Zhao^a Yuting Hu^c Yidun Wan^{a,b,1}

^a*State Key Laboratory of Surface Physics, Department of Physics, Center for Field Theory and Particle Physics, and Institute for Nanoelectronic devices and Quantum computing, Fudan University, Shanghai 200433, China*

^b*Hefei National Laboratory, Hefei 230088, China*

^c*School of Physics, Hangzhou Normal University, Hangzhou 311121, China*

E-mail: yanyanchen235@gmail.com, siyuanwang18@fudan.edu.cn,
yuzhao20@fudan.edu.cn, yuting.phys@gmail.com, ydwan@fudan.edu.cn

ABSTRACT: This paper introduces a novel systematic construction of gapped domain walls (GDWs) within the Levin-Wen (LW) model, advancing our understanding of topological phases. By gluing two LW models along their open sides in a compatible way, we achieve a complete GDW classification by subsets of bulk input data, encompassing e - m exchanging GDWs. A generalized bimodule structure is introduced to capture domain-wall excitations. Furthermore, we demonstrate that folding along any GDW yields a gapped boundary (GB) described by a Frobenius algebra of the input UFC for the folded model, thus bridging GDW and GB classifications within a unified framework.

¹Corresponding author

Contents

1	Introduction	1
2	Motivations and Sketch of Our Approach	2
3	Exactly solvable LW model with GDWs	3
3.1	Definition of $A_1 \overset{\eta}{\dashv} A_2$ -bimodules	5
3.2	Hilbert Space and Hamiltonian	8
3.3	Exact solvability and condition on joining functions	10
4	Ground states and GDW Excitations	11
5	GDWs in the \mathbb{Z}_2 Toric code phase	12
5.1	$\mathcal{C}_1 = \mathcal{C}_2 = \mathcal{R}ep(\mathbb{Z}_2)$	12
5.2	$\mathcal{C}_1 = \mathcal{R}ep(\mathbb{Z}_2)$ and $\mathcal{C}_2 = \mathcal{V}ec(\mathbb{Z}_2)$: Realizing e-m exchange	14
6	GDWs in the doubled Ising phase	16
7	GDWs between the doubled Ising and Toric code phases	17
8	GDW-GB Correspondence	18
9	Conclusions and Outlook	22
A	Review of the LW model	24
A.1	The original LW model	24
A.2	The tailed LW model with enlarged Hilbert space	25
B	Ribbon operators in the bulk	27
B.1	The LW \mathbb{Z}_2 with input $\mathcal{R}ep(\mathbb{Z}_2)$	28
B.2	The LW \mathbb{Z}_2 with input $\mathcal{V}ec(\mathbb{Z}_2)$	29
B.3	The Ising LW	29
C	Exactly solvable conditions to determine B_p^{DW}	31
C.1	Projective condition	31
C.2	Commutative condition	32
D	Excitations in the GDW	34
D.1	Measuring operator at the GDW	34
D.2	Proof of $[B_p^{\text{DW}}, W_{E_1, E_2}^{e-m}] = 0$	34
E	Solutions for joining functions η in specific cases	37
E.1	Case 1: $A_1 = A_2$	37
E.2	Case 2: $A_1 = 1$ or $A_2 = 1$	37

F	Minimal solutions of $A_1 \overset{\eta}{A}_2$-bimodules	38
F.1	$A_1 \overset{\eta}{A}_2$ -bimodules for the LW \mathbb{Z}_2 model	38
F.1.1	$\mathcal{C}_1 = \mathcal{C}_2 = \mathcal{R}ep(\mathbb{Z}_2)$	38
F.1.2	$\mathcal{C}_1 = \mathcal{R}ep(\mathbb{Z}_2), \mathcal{C}_2 = \mathcal{V}ec(\mathbb{Z}_2)$	39
F.2	$A_1 \overset{\eta}{A}_2$ -bimodules for the Ising LW model	40

1 Introduction

Topological phases of matter go beyond the conventional Landau-Ginzburg symmetry breaking paradigm. The study of gapped domain walls (GDWs) of topological phases is crucial to understand the full nature of topological orders, and has potential applications in quantum computing and novel material properties. Although theoretical frameworks like low-energy effective topological quantum field theories (TQFTs) have offered comprehensive understanding for GDWs [1–3], there remains a significant gap between these theories and their realization in actual physical systems. Nonetheless, lattice models of topological orders with GDWs bridge this gap by offering concrete, experimentally relevant models that allow for studying GDWs in greater detail. Previous lattice constructions of GDWs [4–7] have not been universal enough to account for all possible GDWs between two given topological phases, often failing to encompass the e - m exchanging GDWs. Additionally, the tunneling matrix approach [3] offers a complete numerical classification of GDWs, but lacks clear physical insight into their structures.

In this paper, we develop a new way to build GDWs systematically in the framework of the Levin-Wen (LW) model. When we fold a topological system along its GDW, the GDW would become a gapped boundary (GB) of the folded system due to topological invariance. Since the GBs of nonchiral topological phases in 2+1 dimensions have been fully classified in the LW model [8], it is natural to ask the converse question: Can we unfold a topological system with a GB and obtain a GDW between two (not necessarily different) topological phases? We tackle this question by considering two LW models, each having an open side specified by a certain subset of the model’s input data, and sewing the two models along their open sides in a way compatible with the two subsets of input data, such that the resultant model is still gapped, exactly solvable, and topological. The sewed open sides will be a GDW, and different possible ways of sewing yield different types of GDWs.

As such, our key result is a lattice model that can describe all GDWs separating any two LW models with given two input unitary fusion categories (UFCs), therefore offering a unified framework of GDWs for 2+1D topological phases, including e - m exchanging type of GDWs. Additionally, our GDW construction stems from an unfolding process, as we will show that upon folding, a GDW would transform into a GB of the folded phase.

This paper is structured as follows. Section 2 presents the motivation and intuition behind our construction. Section 3 introduces the LW model with GDWs, developing the definition of $A_1 \overset{\eta}{A}_2$ -bimodules and showing that the Hamiltonians of GDWs are classified

by the triples of input data (A_1, A_2, η) . Section 4 constructs creation operators and corresponding measurement operators for the GDWs. Sections 5, 6, and 7 provide concrete examples of our construction. Finally, Section 8 applies the folding trick to our GDW construction, demonstrating its equivalence to an input Frobenius algebra that characterizes a GB of the folded lattice.

2 Motivations and Sketch of Our Approach

A complete understanding of topological orders is impossible without understanding their GBs and GDWs, which also shed new light into topological quantum computation [9–11]. The study of GBs and GDWs is essential for understanding anyon condensation, which exhibits intriguing physical consequences and complex mathematical structures [6, 12–19]. The lattice construction of GDWs in the LW model [4, 5] as defect lines using bimodule categories requires extra input data on top of fusion categories and is difficult to construct interdomain and domain-wall ribbon operators. Furthermore, the recent approach to constructing GDWs through anyon condensation [6] cannot describe e - m exchanging GDWs [20–24]. Here, we take a different approach to construct GDWs in the LW model and offer a classification for GDWs, which includes anyon condensation induced GDWs and e - m exchanging type of GDWs.

Gapped boundaries in the LW model have been completely classified by the Frobenius algebras of the model’s input UFC \mathcal{C} [8]. Hence, a classification of GDWs in the LW model should comply with the classification of GBs in that when the system is folded along a GDW, a GDW would become a GB characterized by certain Frobenius algebra of the input UFC of the folded model. Conversely, suppose we can unfold an open LW model¹ along its GB, we would obtain a model with a GDW. The question is: How can we specify such a GDW?

To tackle this question, we consider two LW models with respectively input UFCs \mathcal{C}_1 and \mathcal{C}_2 , and each model has an open side (not necessarily a GB). We refer to the two models as the \mathcal{C}_1 -model and the \mathcal{C}_2 -model. It is natural to assume that the DOFs on the open side of either model are a subset of the bulk DOFs of the model. We thus specify the two open sides of the two models by algebra objects $A_1 \in \mathcal{C}_1$ and $A_2 \in \mathcal{C}_2$ for the following reason. We want to make our model as general as possible, so minimal assumptions should be imposed on the data specifying the open sides. It is then natural to choose algebra objects—the simplest yet interesting structures—in the input UFCs. Now we try to glue the two models along their open sides as follows. We devise a joining function $\eta : A_1 \times A_2 \rightarrow \mathbb{C}$, which dictates how the DOFs taking value in A_1 are coupled with those taking value in A_2 . A compatibility check of this gluing is that when the \mathcal{C}_2 -model (\mathcal{C}_1 -model) describes a trivial phase, A_1 (A_2) should be a Frobenius algebra object in \mathcal{C}_1 (\mathcal{C}_2) and characterizes the GB of the \mathcal{C}_1 -model (\mathcal{C}_2 -model).

Now, to ensure that the gluing process of two open sides results in a GDW, we should construct a proper Hamiltonian to describe the glued sides. We take the tailed LW model defined in [25] because it has an enlarged Hilbert space that encompasses the full anyon

¹An open LW model means a LW model with a GB.

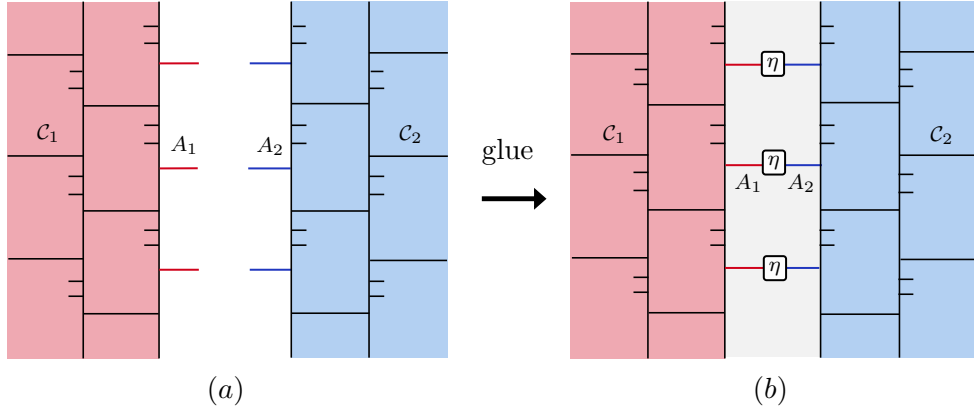


Figure 1. The gluing process. (a) Part of the lattice of the \mathcal{C}_1 -model and that of the \mathcal{C}_2 -model. Their open sides are characterized by A_1 and A_2 , respectively.

spectra of the topological phases it describes. Based on this model, we construct the Hamiltonian of the glued sides, such that it is exactly solvable and gapped. This construction unravels the function η that joins the algebras A_1 and A_2 characterizing the two open sides. A tuple (A_1, A_2, η) uniquely specifies a GDW.

As shown in Section 3, upon joining two open edges, new DOFs inevitably emerge at the joining point. Such new DOFs form generalized bimodules of A_1 and A_2 —dubbed $A_1 \overset{\eta}{\boxtimes} A_2$ -bimodules—to be defined in Section 3.1. Given a GDW specified by (A_1, A_2, η) , quasiparticles on the GDW are in one-to-one correspondence with $A_1 \overset{\eta}{\boxtimes} A_2$ -bimodules.

We also perform a consistency check of our construction as follows. Suppose we have constructed a model comprising a \mathcal{C}_1 -model and a \mathcal{C}_2 model sandwiching a GDW specified by (A_1, A_2, η) . We show that folding this model along its GDW results in a $\mathcal{C}_1^{\text{op}} \boxtimes \mathcal{C}_2$ -model with a GB specified by the Frobenius algebra object $A_1^{\text{op}} \times_{\eta} A_2$ in $\mathcal{C}_1^{\text{op}} \boxtimes \mathcal{C}_2$. Therefore, our construction of GDWs in the LW model can be regarded as a way of unfolding the $\mathcal{C}_1^{\text{op}} \boxtimes \mathcal{C}_2$ -model with a GB along the GB. This may inspire attempts in unfolding a non-chiral topological phase along its GB to realize a lattice model of chiral topological orders.

3 Exactly solvable LW model with GDWs

The tailed Levin-Wen (LW) model [25] is defined on a two-dimensional trivalent lattice (see Fig. 2) with oriented edges and tails (dangling edges). The lattice consists of two types of vertices: **primary vertices**, which are trivalent with three incident edges, and **secondary vertices**, which have two incident edges and one tail. Each tail is associated with its nearest primary vertex. Residing on each edge/tail is a DOF taking value in a finite set L of labels that label the representative simple objects in a fusion category \mathcal{C} —the input fusion category of the model. We refer to this construction as the \mathcal{C} -model. The Hilbert space of the model is spanned by all possible label assignments to the edges and tails, subject to the constraint that the three labels meeting at any vertex must satisfy the fusion rules of \mathcal{C} .

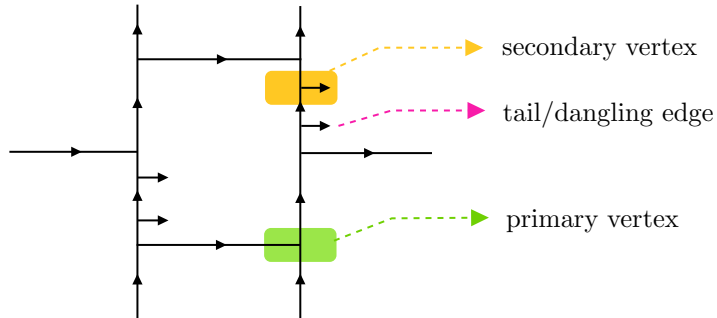


Figure 2. The tailed LW model. The primary and secondary vertices are highlighted in the lattice.

The Hamiltonian of the model is the sum over all primary-vertex operators and plaquette operators.

$$H = - \sum_v A_v - \sum_p B_p. \quad (3.1)$$

Detailed explanation of the Hamiltonian can be found in Appendix A.2. Here is a brief account. Each primary-vertex operator A_v is a projector that acts on a primary vertex v . The action of A_v returns 1 if the label on the tail associated with v is 1—the trivial object of \mathcal{C} —otherwise, it vanishes. The plaquette operator B_p is also a projector. All operators A_v and B_p commute with one another, such that the Hamiltonian is exactly solvable. A ground state of the system is a common eigenstate of all A_v and B_p with eigenvalue +1. In an excited state, however, the action of one or more A_v and/or B_p operators would return 0. As mentioned already, if the action of an A_v returns 0, a chargeon is said to reside on the tail associated with v . If the action of a B_p returns 0, a fluxon resides in plaquette p . If both the actions of a B_p and an A_v (with v 's tail in p) return 0, a dyon inhabits in plaquette p .

We now cut the \mathcal{C} -model open vertically along edges and remove the part of the lattice to the right of and including the edges on the cut. This results in a model with an open side consisting of open edges (which should not be confused with tails in the bulk). The question arises: What are the DOFs on the open edges? It is known that if the open side is a GB, the DOFs on the open edges take values in a Frobenius algebra object in \mathcal{C} . This is referred to as the GB condition[8, 26] or the Frobenius condition[27]. But our open side is not necessarily a GB, so it is reasonable to relax the Frobenius condition. We then assume that the DOFs on our open edges take value in an algebra object A in \mathcal{C} defined as a pair $A = (L_A, f)$, where $L_A \subseteq L$, and $f : L_A^3 \rightarrow \mathbb{C}$ is the algebra multiplication satisfying the defining properties:

$$\begin{aligned} \text{unit} \quad & f_{bb^*1} = f_{b1b^*} = f_{1bb^*} = 1, \forall b \in L_A \\ \text{cyclic} \quad & f_{abc} = f_{cab}. \end{aligned} \quad (3.2)$$

We assume algebra A is multiplicity free. Each open edge carries an element of L_A .

Next, given two fusion categories \mathcal{C}_1 and \mathcal{C}_2 , with respectively label sets L_1 and L_2 , consider the \mathcal{C}_1 -model and \mathcal{C}_2 , each having an open side. See Fig. 1(a). The open side of the \mathcal{C}_1 -model (\mathcal{C}_2 -model) is specified by the algebra objects (L_{A_1}, f) ((L_{A_2}, g)), with f (g)

being the algebra multiplication defined by Eq. (3.2). In this paper, we focus on the case where \mathcal{C}_2 is a subcategory of \mathcal{C}_1 . We leave more general cases for future work.

We are ready to glue the \mathcal{C}_1 -model and \mathcal{C}_2 -model along their open sides by joining the open edges head to head horizontally as seen in Fig. 1(b). We devise a joining function $\eta : A_1 \times A_2 \rightarrow \mathbb{C}$ that dictates joining two open edges: If $\eta_{ab} \neq 0$ for $a \in L_{A_1}$ and $b \in L_{A_2}$, the two open edges can be joined; otherwise, the joining is disallowed.

The total Hilbert space of the glued model contains only those states on the glued lattice with all open edges joined pairwise. See Fig. 1(b) for illustration. The glued lattice now has three regions: a vertical strip (grey in the figure) of plaquettes in the middle, which is to be proven as a GDW of the glued model, the original bulk of the \mathcal{C}_1 -model on the left (red in the figure), and that of the \mathcal{C}_2 -model on the right (blue in the figure). We will provide consistency conditions that determine all possible joining functions for given algebras A_1 and A_2 . Each tuple (A_1, A_2, η) specifies a GDW in the glued model. Hence, a glued model's input data is a 5-tuple $(\mathcal{C}_1, \mathcal{C}_2, A_1, A_2, \eta)$.

At this point, for a glued model with input data $(\mathcal{C}_1, \mathcal{C}_2, A_1, A_2, \eta)$, its total Hilbert space is spanned by configurations of all possible assignments of labels to the bulk edges (in black) on both sides of the GDW, pertaining to the fusion rules, and labels to the joined open edges (red line segments for the \mathcal{C}_1 -model and blue for the \mathcal{C}_2 -model) pertaining to the joining function η , which is symbolized by a square box in the figure 1(b). Nevertheless, this Hilbert space is insufficient to encompass quasiparticle excitations on the GDW, which have been shown to exist on the GDW between two topological phases, as well as on the GB of a topological phase[25]. This insufficiency is due to that the DOFs on any two joined open edges are fully determined by the input joining function η . We thus need to enlarge the Hilbert space by introducing new DOFs to the GDW in the glued model to describe possible quasiparticle excitations on the GDW. But how?

A clue can be drawn from the case of the LW model with a GB, which is characterized by a Frobenius algebra object of the model's input fusion category. In this case, the quasiparticles on the GB carry the bimodules of the Frobenius algebra. Coming back to our construction, it is then reasonable to guess that the quasiparticles on a GDW specified by (A_1, A_2, η) carry certain bimodules acted on by both A_1 and A_2 in a way pertaining to η . Indeed, by constructing the quasiparticle creation operators (see Section 4) on our GDW, we can show that GDW quasiparticles do carry what we call $A_1 \overset{\eta}{A_2}$ -bimodules, a generalized type of algebra bimodules. This finding motivates us to introduce new DOFs capturing such bimodules in the glued region of our lattice, such that the model's Hilbert space can encompass GDW quasiparticles in the first place.

To see how new DOFs would be introduced in the GDW, we first need to define $A_1 \overset{\eta}{A_2}$ -bimodules as follows.

3.1 Definition of $A_1 \overset{\eta}{A_2}$ -bimodules

Consider two UFCs $\mathcal{C}_1, \mathcal{C}_2$ and two algebras $A_1 \in \mathcal{C}_1, A_2 \in \mathcal{C}_2$. Let the set of all representative simple objects of $\mathcal{C}_1, \mathcal{C}_2, A_1, A_2$ be $L_1, L_2, L_{A_1}, L_{A_2}$, respectively. Given a joining

function $\eta : A_1 \times A_2 \rightarrow \mathbb{C}$, we can define a set

$$L_\eta = \{(a, b) | \eta_{ab} \neq 0, a \in L_{A_1}, b \in L_{A_2}\} \quad (3.3)$$

to label the pairs of objects in L_{A_1} and L_{A_2} that are allowed by η . For convenience, we set a characteristic function $\Delta : \mathbb{C} \rightarrow \{0, 1\}$ for η :

$$\Delta(x) = \begin{cases} 0, & x = 0; \\ 1, & x \neq 0. \end{cases} \quad (3.4)$$

We shall consider, without loss of generality, two scenarios: (1) \mathcal{C}_2 is a subcategory of \mathcal{C}_1 , then $L_2 \subset L_1$ and all other data of \mathcal{C}_2 are embedded in those of \mathcal{C}_1 . (2) \mathcal{C}_2 is not a subcategory of \mathcal{C}_1 , but the objects and morphisms of \mathcal{C}_2 can be represented by those of \mathcal{C}_1 . For instance, when \mathcal{C}_1 is Morita equivalent to \mathcal{C}_2 (e.g. $\mathcal{R}ep(\mathbb{Z}_1)$ and $\mathcal{V}ec(\mathbb{Z}_2)$), one can establish isomorphic maps between their input data. Then, we define $A_1 \overset{\eta}{\dashv} A_2$ -bimodules as follows.

An $A_1 \overset{\eta}{\dashv} A_2$ -bimodule M is a pair (L_M, P_M) , where $L_M \subseteq L_1$, and P_M is a set of action tensors $[P_M]_{imj}^{ab}$ labeled by $(a, b) \in L_\eta$ and tensorial indices $i, j \in L_M, m \in L_1$, satisfying the following equation:

The diagram shows two equivalent representations of a stacked action tensor. On the left, two P_M boxes are stacked vertically. The bottom box has an incoming red arrow from the left labeled a_1 and an outgoing blue arrow to the right labeled b_1 . The top box has an incoming red arrow from the left labeled a_2 and an outgoing blue arrow to the right labeled b_2 . A vertical arrow labeled s_1 points up from the bottom box to the top box. A vertical arrow labeled s_3 points up from the top box. On the right, a single P_M box has a thick red dot at its left vertex where two red arrows labeled a_1 and a_2 meet. A thick blue dot is at its right vertex where two blue arrows labeled b_1 and b_2 meet. A vertical arrow labeled s_1 points up into the bottom vertex, and a vertical arrow labeled s_3 points up from the top vertex. The two diagrams are equated with the coefficient $\Delta(\eta_{a_1 b_1} \eta_{a_2 b_2} \eta_{a_3 b_3})$.

In Eq. (3.5) and hereafter, the box labeled by P_M encapsulates the corresponding action tensor:

The diagram shows a P_M box with an incoming red arrow from the left labeled a and an outgoing blue arrow to the right labeled b . A vertical arrow labeled s_1 points up into the bottom vertex, and a vertical arrow labeled s_2 points up from the top vertex. This is equated to a summation over $m \in L_1$ of the coefficient $[P_M]_{s_1 m s_2}^{ab}$ multiplied by a diagram where a red arrow labeled a and a blue arrow labeled b meet at a vertex with a thick red dot. A vertical arrow labeled s_1 points up into this vertex, and a vertical arrow labeled s_2 points up from another vertex where a blue arrow labeled m meets the red arrow.

where $s_1, s_2 \in L_M$, and $m \in L_1$.

In Eq. (3.5) and hereafter, a thickened edge indicates a summation over all values of this edge's DOF, while a thick red (blue) dot at a vertex absorbs the algebra multiplication f (g) for A_1 (A_2):

The diagram shows two equations. The first shows a vertex with a thick red dot where a red arrow labeled a and a red arrow labeled b meet, and a red arrow labeled c points up. This is equated to f_{abc} times a vertex where a red arrow labeled a and a red arrow labeled b meet, and a red arrow labeled c points up. The second equation shows a vertex with a thick blue dot where a blue arrow labeled a and a blue arrow labeled b meet, and a blue arrow labeled c points up. This is equated to g_{abc} times a vertex where a blue arrow labeled a and a blue arrow labeled b meet, and a blue arrow labeled c points up.

The Eq. (3.5) indicates the equivalence between $A_1 \otimes (A_1 \otimes M \otimes A_2) \otimes A_2$ and $(A_1 \otimes A_1) \otimes M \otimes (A_2 \otimes A_2)$. We can transform the basis on the LHS to that on the RHS by a

series of F-moves in the following:

$$\begin{array}{c} i \\ \swarrow \\ m \\ \searrow \\ j \\ \swarrow \quad \searrow \\ k \quad l \end{array} = \sum_{n \in L} G_{kln}^{jim} v_m v_n \begin{array}{c} i \quad j \\ \swarrow \quad \searrow \\ n \\ \swarrow \quad \searrow \\ k \quad l \end{array}, \quad (3.8)$$

$$\begin{array}{c} a_1 \\ \swarrow \\ m \\ \searrow \\ j \\ \swarrow \quad \searrow \\ a_2 \quad l \end{array} = \sum_{n \in L_{A_1}} G_{a_2 l a_3}^{j a_1 m} v_m v_{a_3} \begin{array}{c} a_1 \quad j \\ \swarrow \quad \searrow \\ a_3 \\ \swarrow \quad \searrow \\ a_2 \quad l \end{array}, \quad (3.9)$$

$$\begin{array}{c} i \\ \swarrow \\ m \\ \searrow \\ b_1 \\ \swarrow \quad \searrow \\ k \quad b_2 \end{array} = \sum_{n \in L_{A_2}} G_{k b_2 b_3}^{b_1 i m} v_m v_{b_3} \begin{array}{c} i \quad b_1 \\ \swarrow \quad \searrow \\ b_3 \\ \swarrow \quad \searrow \\ k \quad b_2 \end{array}. \quad (3.10)$$

Then, comparing the linear combination coefficients on both sides of Eq. (3.5) yields the following tensor equation:

$$\sum_{\substack{a_3 \in L_{A_1}, b_3 \in L_{A_2} \\ s_2 \in L_M, l, m, n \in L_1}} P_{s_1 m s_2}^{a_1 b_1} P_{s_2 n s_3}^{a_2 b_2} G_{b_2 n s_2}^{a_1 m l} G_{s_3 a_2 n}^{a_1 l a_3} G_{b_2 l m}^{s_1 b_1 b_3} v_l v_m v_n v_{s_2} v_{a_3} v_{b_3} \\ = \sum_{\substack{a_3 \in L_{A_1}, b_3 \in L_{A_2} \\ l \in L_1}} \Delta(\eta_{a_1 b_1} \eta_{a_2 b_2} \eta_{a_3 b_3}) P_{s_1 l s_3}^{a_3 b_3} f_{a_2 a_1 a_3} g_{b_1 b_2 b_3}, \quad (3.11)$$

for $a_1, a_2 \in L_{A_1}$, $b_1, b_2 \in L_{A_2}$.

An $A_1 \overset{\eta}{-} A_2$ -bimodule is, in general, not a A_1 - A_2 -bimodule as defined in [8], but a generalization thereof. Unlike A_1 - A_2 -bimodules, an $A_1 \overset{\eta}{-} A_2$ -bimodule is not necessarily both a left A_1 -module and right A_2 -module. Nonetheless, when $\Delta(\eta_{ab}) = 1$ for any $a \in A_1, b \in A_2$, Eq. (3.11) reduces to the defining equation of A_1 - A_2 -bimodules.

The $A_1 \overset{\eta}{-} A_2$ -bimodules satisfy the following orthonormality condition:

$$\mathcal{T} \left(\begin{array}{c} \xrightarrow{a_1} \\ \uparrow s \\ \boxed{P_M} \\ \downarrow s \\ \boxed{P_N} \\ \uparrow s \\ \xrightarrow{b_1} \end{array} \right) = \delta_{M,N} \Delta(\eta_{a_1 b_1} \eta_{a_2 b_2} \eta_{a_3 b_3}) \frac{d_{A_1} d_{A_2} d_s}{d_M} \left(\begin{array}{c} \xrightarrow{a_1} \\ \uparrow s \\ \boxed{P_M} \\ \downarrow s \\ \xrightarrow{b_1} \end{array} \right), \quad (3.12)$$

where $d_M = \sum_{s \in L_M} d_s$ and $d_A = \sum_{a \in A} d_a$.

We package the three black edges that describe the DOFs before and after the action of A_1 and A_2 into a filled box. As shown in Eq. (3.13), the filled box associated with an arbitrary $A_1 \overset{\eta}{-} A_2$ -bimodule M can be rigorously expanded as a linear combination of basis

states, which explicitly capture the internal DOFs in the filled box.

$$\left(\begin{array}{c} a \xrightarrow{M} b \\ \blacksquare \end{array} \right) = \sum_{s_1, s_2 \in L_M} \frac{u_{s_1} u_{s_2}}{u_a u_b} \left(\begin{array}{c} a \xrightarrow{P_M} b \\ \uparrow s_2 \\ \blacksquare \\ \uparrow s_1 \end{array} \right), \quad (3.13)$$

where $u_i = (d_i)^{\frac{1}{4}}$ and d_i is the quantum dimension of the string type i . In cases where the trivial $A_1 \overset{\eta}{A_2}$ -bimodule M_0 is explicitly required, we use an unfilled square box to avoid ambiguity.

The trivial $A_1 \overset{\eta}{A_2}$ -bimodule M_0 is a pair (L_{M_0}, P_{M_0}) , where L_{M_0} contains $1 \in L_1$, and the action tensors satisfying

$$[P_{M_0}]_{1m1}^{ab} = \delta_{a,m} \delta_{b,m}, \quad (3.14)$$

which indicates that the trivial anyon in the bulk would be identified as M_0 in the GDW.

3.2 Hilbert Space and Hamiltonian

To enlarge the Hilbert space, such that it can bear quasiparticle excitations along the DW, we dress each gluing point by a filled square box as a new DOF, taking value in the simple (i.e., irreducible) $A_1 \overset{\eta}{A_2}$ bimodules, as shown in Fig. 3. The enlarged Hilbert space is then spanned by all possible configurations (subject to fusion rules at all vertices) of the simple objects of the input UFCs \mathcal{C}_1 and \mathcal{C}_2 on the bulk edges, the basis elements of the algebras A_1 and A_2 on the DW edges, and the simple $A_1 \overset{\eta}{A_2}$ bimodules $\{M_0, M_1, M_2, \dots\}$ on the filled square boxes.

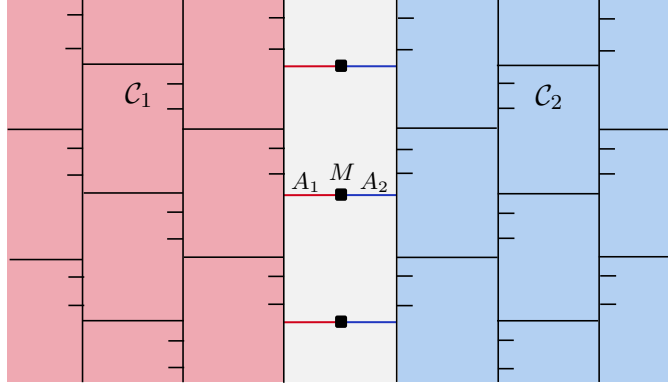


Figure 3. Two extended LW models (red and blue) with input fusion categories \mathcal{C}_1 and \mathcal{C}_2 , joint by a DW (light grey). The joining points, bearing the algebraic actions of A_1 and A_2 , are characterized by the $A_1 \overset{\eta}{A_2}$ -bimodules M .

For the tailed LW model with the DW shown in Fig. 3, the modified Hamiltonian from (3.1) is given by:

$$H = - \sum_{v \text{ in bulk}} A_v^{\text{bulk}} - \sum_{p \text{ in bulk}} B_p^{\text{bulk}} - \sum_{v \text{ in DW}} A_v^{\text{DW}} - \sum_{p \text{ in DW}} B_p^{\text{DW}}. \quad (3.15)$$

The operators involved in the Hamiltonian are explained as follows. Any primary vertex with black incident edges is a bulk vertex, and one with a colored incident edge is a DW vertex. Bulk and DW plaquettes are obvious. The actions of the bulk operators A_v^{bulk} and B_p^{bulk} of the \mathcal{C}_1 -model and the \mathcal{C}_2 -model are given in Appendix A.2.

Then the vertex operators for the vertices in the GDW are given as follows:

$$A_v^{\text{DW}} \left| \begin{array}{c} k_2 \uparrow \\ q \leftarrow k_1 \\ i \nearrow k_1 \\ j \searrow \end{array} \right\rangle = \delta_{q,0} \left| \begin{array}{c} k_2 \uparrow \\ q \leftarrow k_1 \\ i \nearrow k_1 \\ j \searrow \end{array} \right\rangle, \quad A_v^{\text{DW}} \left| \begin{array}{c} k_2 \uparrow \\ k_1 \rightarrow q \\ i \nearrow k_1 \\ j \searrow \end{array} \right\rangle = \delta_{q,0} \left| \begin{array}{c} k_2 \uparrow \\ k_1 \rightarrow q \\ i \nearrow k_1 \\ j \searrow \end{array} \right\rangle. \quad (3.16)$$

Plaquette operators on the GDW is defined as

$$B_p^{\text{DW}} = \sum_{s \in A_1, t \in A_2} v_s v_t (\eta_{st})^2 B_p^{st}, \quad (3.17)$$

where $v_i = \sqrt{d_i}$ with d_i the quantum dimension of i . An operator B_p^{st} acts on a DW plaquette by inserting a bicolored loop in plaquette p and fusing the loop with p 's boundary edges. This action is given as follows.

$$\begin{aligned} B_p^{st} \left| \begin{array}{c} k_1 \uparrow \\ i_1 \rightarrow M_0 \rightarrow j_1 \uparrow l_1 \\ i_2 \uparrow \\ k_2 \rightarrow \\ i_3 \uparrow \\ i_4 \rightarrow M_1 \rightarrow j_4 \uparrow l_3 \\ k_3 \uparrow \end{array} \right\rangle &= \delta_{M_0, M_1} \Delta(\eta_{i_1 j_1} \eta_{i_4 j_4}) \left| \begin{array}{c} k_1 \uparrow \\ i_1 \rightarrow M_0 \rightarrow j_1 \uparrow l_1 \\ i_2 \uparrow \\ k_2 \rightarrow \\ i_3 \uparrow \\ i_4 \rightarrow M_1 \rightarrow j_4 \uparrow l_3 \\ k_3 \uparrow \end{array} \right\rangle \\ &= \sum_{\substack{i'_1, i'_2, i'_3, i'_4 \in A_1 \\ j'_1, j'_2, j'_3, j'_4 \in A_2}} \Delta(\eta_{i_1 j_1} \eta_{i_4, j_4} \eta_{i'_1 j'_1} \eta_{j'_4 j'_4}) u_{i_1} u_{j_1} u_{i_4} u_{j_4} u_{i'_1} u_{j'_1} u_{i'_4} u_{j'_4} v_{i_2} v_{j_2} \\ &\quad \times v_{i_3} v_{j_3} v_{i'_2} v_{j'_2} v_{i'_3} v_{j'_3} G_{k_1 i_2 i'_2}^{s* i'_1 i_1} G_{k_2 i_3 i'_3}^{s* i'_2 i_2} G_{k_3 i_4 i'_4}^{s* i'_3 i_3} G_{l_3 j_3 j'_3}^{t* j'_4 j_4} G_{l_2 j_2 j'_2}^{t* j'_3 j_3} \\ &\quad \times G_{l_1 j_1 j'_1}^{t* j'_2 j_2} f_{s i'_1 i_1} f_{s i'_4 i_4} g_{t j'_1 j_1} g_{t j_4 j'_4} \left| \begin{array}{c} k_1 \uparrow \\ i'_1 \rightarrow M_0 \rightarrow j'_1 \uparrow l_1 \\ i'_2 \uparrow \\ k_2 \rightarrow \\ i'_3 \uparrow \\ i'_4 \rightarrow M_1 \rightarrow j'_4 \uparrow l_3 \\ k_3 \uparrow \end{array} \right\rangle. \end{aligned} \quad (3.18)$$

In the derivation above, as a simplification, we moved any tail attached to p 's boundary edges away using F-moves Eqs. (3.8)–(3.10), such that the computation involves no tails. Equation (3.18) implies that DW plaquette operators project out states where filled square boxes in the DW carry non-trivial $A_1 \overset{\eta}{\dashv} A_2$ -bimodules.

The derivation of the plaquette operators needs the Pachner moves in the GDW, which

has not been defined yet. Here, we propose the Pacher moves at the GDW as follows:

$$\mathcal{T} \left| \begin{array}{c} j' \quad M \quad j \\ \text{---} \text{---} \text{---} \\ \text{---} \text{---} \text{---} \\ i' \quad M \quad i \end{array} \right\rangle = \Delta[\eta_{j'j}\eta_{i'i}\eta_{k'k}] \frac{u_{i'}u_{j'}u_iu_j}{u_ku_{k'}} f_{i'j'k'^*} g_{j^*i^*k} \left| \begin{array}{c} k' \quad M \quad k \\ \text{---} \text{---} \text{---} \\ \text{---} \text{---} \text{---} \\ i' \quad M \quad i \end{array} \right\rangle, \quad (3.19)$$

$$\mathcal{T} \left| \begin{array}{c} k' \quad M \quad k \\ \text{---} \text{---} \text{---} \\ \text{---} \text{---} \text{---} \\ i' \quad M \quad i \end{array} \right\rangle = \sum_{\substack{i',j' \in A_1 \\ i,j \in A_2}} \Delta[\eta_{j'j}\eta_{i'i}\eta_{k'k}] \frac{u_{i'}u_{j'}u_iu_j}{u_ku_{k'}} f_{i'j'k'^*} g_{j^*i^*k} \left| \begin{array}{c} j' \quad M \quad j \\ \text{---} \text{---} \text{---} \\ \text{---} \text{---} \text{---} \\ i' \quad M \quad i \end{array} \right\rangle. \quad (3.20)$$

Equation (3.19) is equivalent to the defining equation (3.5) of $A_1 \overset{\eta}{\dashv} A_2$ -bimodules.

We have not yet discussed which joining functions are appropriate to guarantee compatibility between the DW and the adjacent \mathcal{C}_1 -model and \mathcal{C}_2 -model. We now tackle this problem to derive all possible joining functions.

3.3 Exact solvability and condition on joining functions

In order that the model is exactly solvable, we require the operators in the DW to commute among themselves and with bulk operators. Domain-wall operators by definition commute with all bulk operators. Domain-wall vertex operators also commute with themselves and with DW plaquette operators. The commutativity between two neighboring DW plaquette operators is nontrivial and leads to the following condition:

$$\sum_{\substack{k_2, k'_2 \in A_1 \\ l_2, l'_2 \in A_2}} \sum_{\substack{\eta_{i_1 j_1}, \eta_{i_2 j_2}, \eta_{k_1 l_1}, \\ \eta_{k_2 l_2}, \eta_{k_3 l_3} \neq 0}} G_{k_1^* i_1^* k_2^*}^{k_3 i_2 k_2^*} G_{j_2^* l_3^* l_2^*}^{j_1 l_1 l_2^*} v_{l_2} v_{l'_2} v_{k_2} v_{k'_2} f_{k_2^* k_3 i_2} f_{k_1^* i_1^* k_2} g_{l_2^* j_1 l_1} g_{l_3^* l_2 j_2^*} \\ = \sum_{\substack{k'_2 \in A_1 \\ l'_2 \in A_1}} \sum_{\substack{\eta_{i_1 j_1}, \eta_{i_2 j_2}, \eta_{k_1 l_1}, \\ \eta_{k_2 l'_2}, \eta_{k_3 l_3} \neq 0}} f_{k'_2 i_1^* k_3} f_{k_1^* k'_2 i_2} g_{l'_2 i_1 j_2^*} g_{l_3^* j_1 l'_2}, \quad (3.21)$$

which can be presented graphically as:

$$\mathcal{T} \left| \begin{array}{c} i_1 \quad j_1 \\ \text{---} \text{---} \text{---} \\ \text{---} \text{---} \text{---} \\ i_2 \quad j_2 \end{array} \right\rangle = \Delta[\eta_{i_1 j_1} \eta_{i_2 j_2} \eta_{k_1 l_1} \eta_{k_3 l_3}] \left| \begin{array}{c} i_1 \quad j_1 \\ \text{---} \text{---} \text{---} \\ \text{---} \text{---} \text{---} \\ i_2 \quad j_2 \end{array} \right\rangle, \quad (3.22)$$

Vertex operators A_v and plaquette operators B_p in the original LW model are projectors, which detect whether an anyon excitation exists where such an operator acts. As we now extend the LW model to the case with GDW, we also require all DW operators to be projectors. Domain-wall vertex operators A_v^{DW} are projectors by definition. Demanding DW plaquette operators B_p^{DW} to be projectors results in the following condition on the joining function η :

$$\sum_{\substack{i', j' \in \bar{A} \\ i, j \in A}} \sum_{\substack{\eta_{i'i}, \eta_{j'j}, \\ \eta_{k'k} \neq 0}} \delta_{i'j'k'} \delta_{ijk} \frac{v_{i'}v_{j'}v_i v_j}{v_k v_{k'}} f_{i'^* j'^* k'^*} f_{j'i'k'^*} g_{j i k^*} g_{i^* j^* k} (\eta_{j'j} \eta_{i'i})^2 = (\eta_{k'k})^2, \quad (3.23)$$

See Appendix C for the derivation of (3.21) and (3.23). Appendix E shows the solutions of the joining functions η in certain cases. We find that even when \mathcal{C}_1 and \mathcal{C}_2 are fundamentally different, there still exist solutions for η that physically connect the GBs of the \mathcal{C}_1 -model and the \mathcal{C}_2 -model. In this case, A_1 and A_2 should be Frobenius algebra objects in \mathcal{C}_1 and \mathcal{C}_2 , respectively, indicating that the GDW is the vacuum.

Now that our Hamiltonian (3.15) consists of commuting projectors, the system is gapped. The ground-state Hilbert space is topologically protected, in the sense that it is invariant under the Pachner moves. Hence, our Hamiltonian (3.15) defines a composite system of two LW models separated by a GDW. A GDW between two LW models with input UFCs \mathcal{C}_1 and \mathcal{C}_2 is specified by a triple (A_1, A_2, η) , where A_1 (A_2) is an algebra object of \mathcal{C}_1 (\mathcal{C}_2), and η is a pairing function of the two algebras.

4 Ground states and GDW Excitations

The ground states of the tailed LW model with GDWs are the +1 eigenvectors of all vertex operators and plaquette operators in the Hamiltonian (3.15). Therefore, in a ground state, the tails in Fig. 3 are all trivial and the boxes at the gluing points are all labeled by the trivial $A_1 \overset{\eta}{-} A_2$ -bimodule M_0 . For the ground states, an edge along the left (right) boundary of the GDW region becomes a right A_1 -module in \mathcal{C}_1 (left A_2 -module in \mathcal{C}_2). A right A_1 -module (left A_2 -module) in \mathcal{C}_1 (\mathcal{C}_2) is a subset $L_{\text{RMod}_{A_1}(\mathcal{C}_1)} \subset L$ ($L_{\text{LMod}_{A_2}(\mathcal{C}_2)} \subset L$) equipped with a right (left) action tensor $[\rho_1]_{i_1 i_2}^{a_1}$ ($[\rho_2]_{j_1 j_2}^{b_1}$) satisfying the following equations:

$$\mathcal{T} \left| \begin{array}{c} \uparrow i_2 \\ \boxed{\rho_1} \\ \uparrow i_1 \end{array} \right. \begin{array}{c} \rightarrow a_2 \\ \rightarrow a_1 \end{array} \rangle = \left| \begin{array}{c} \uparrow i_2 \\ \boxed{\rho_1} \\ \uparrow i_1 \end{array} \right. \begin{array}{c} \rightarrow a_2 \\ \rightarrow a_1 \end{array} \rangle, \quad \mathcal{T} \left| \begin{array}{c} \uparrow j_2 \\ \boxed{\rho_2} \\ \uparrow j_1 \end{array} \right. \begin{array}{c} \rightarrow b_2 \\ \rightarrow b_1 \end{array} \rangle = \left| \begin{array}{c} \uparrow j_2 \\ \boxed{\rho_2} \\ \uparrow j_1 \end{array} \right. \begin{array}{c} \rightarrow b_2 \\ \rightarrow b_1 \end{array} \rangle. \quad (4.1)$$

In the tailed LW model, the elementary excitations (dyon species) are endowed with topological symmetries², which can be characterized by irreducible solutions of half-braiding tensors in Appendix B.

At the GDW, elementary excitations are characterized by irreducible $A_1 \overset{\eta}{-} A_2$ -bimodules. GDW quasiparticles can be pairwise created by the following creation operator:

$$W_M^{\text{gp1}} \left| \begin{array}{c} \boxed{\rho_1} \\ \boxed{\rho_1} \\ \boxed{\rho_1} \end{array} \right. \begin{array}{c} \rightarrow p_1 \\ \rightarrow M_0 \\ \rightarrow p_2 \end{array} \begin{array}{c} \leftarrow p_2 \\ \leftarrow M \\ \leftarrow p_1 \end{array} \boxed{\rho_2} \rangle = \left| \begin{array}{c} \boxed{\rho_1} \\ \boxed{\rho_1} \\ \boxed{\rho_1} \end{array} \right. \begin{array}{c} \rightarrow p_1 \\ \rightarrow M \\ \rightarrow p_2 \end{array} \begin{array}{c} \leftarrow p_2 \\ \leftarrow M \\ \leftarrow p_1 \end{array} \boxed{\rho_2} \rangle. \quad (4.2)$$

²The elementary excitations are identified with irreducible representations of the tube algebra [25].

Here, the state on the LHS with all M_0 at the GDW indicates the absence of quasiparticle excitations at the GDW. The action of $W_M^{\text{gp}_1}$ replaces the unfilled square box at the gluing point gp_1 by a filled square box associated with an irreducible $A_1 \overset{\eta}{\dashv} A_2$ -bimodule M . As a result, a pair of quasiparticles of the same type, characterizing by the $A_1 \overset{\eta}{\dashv} A_2$ -bimodule M , are created in the neighboring plaquettes p_1 and p_2 sharing the gluing point gp_1 in the GDW.

To detect these quasiparticles, we introduce the measurement operator $\Pi_M^{p_1}$, which acts as a projector on the excited state with a quasiparticle of type M in the GDW plaquette p_1 . More detailed derivation is given in Appendix D.1.

In the next sections, we will discuss some archetypal examples to elaborate our construction.

5 GDWs in the \mathbb{Z}_2 Toric code phase

In this section, we produce all the GDWs that separate the two toric code phases. Notably, the e - m exchanging GDWs can be realized in our GDW construction framework, without inserting additional σ defects or introducing lattice dislocalization. This method is also applicable to studying e - m exchanging GDWs between the different LW models, such as those with input UFCs $\mathcal{R}ep(\mathbb{Z}_n)$ and $\mathcal{V}ec(\mathbb{Z}_n)$.

5.1 $\mathcal{C}_1 = \mathcal{C}_2 = \mathcal{R}ep(\mathbb{Z}_2)$

Here we consider two \mathbb{Z}_2 LW models separated by a GDW. The input fusion category here is $\mathcal{R}ep(\mathbb{Z}_2)$, which has two self-dual simple objects 1 and ψ , with $d_1 = d_\psi = 1$. The fusion rules are $\delta_{111} = \delta_{1\psi\psi} = 1$. The $6j$ -symbols are $G_{kln}^{ijm} = \delta_{ijm}\delta_{klm^*}\delta_{jkn^*}\delta_{inl}$. Table 1 records all possible triples (A_1, A_2, η) :

Plugging the five solutions in Table 1 into the defining equation (3.17) of DW plaquette operators, we obtain five distinct DW plaquette operators:

$$\begin{aligned}
 B_p^{\text{DW}_1} &= B_p^{11}, & B_p^{\text{DW}_2} &= \frac{B_p^{11} + B_p^{1\psi}}{2}, & B_p^{\text{DW}_3} &= \frac{B_p^{11} + B_p^{\psi 1}}{2}, \\
 B_p^{\text{DW}_4} &= \frac{B_p^{11} + B_p^{1\psi} + B_p^{\psi 1} + B_p^{\psi\psi}}{4}, & B_p^{\text{DW}_5} &= \frac{B_p^{11} + B_p^{\psi\psi}}{2}.
 \end{aligned} \tag{5.1}$$

We observe that the fifth DW plaquette operator $B_p^{\text{DW}_5}$ coincides with the bulk plaquette operator B_p^{bulk} , so the corresponding GDW is trivial: The system is just a single \mathbb{Z}_2 toric code phase without any domain wall. The other four DW plaquette operators

$A_1 \backslash A_2$	1	$1 \oplus \psi$
1	(1) $\eta_{11} = 1$	(2) $\eta_{11} = \eta_{1\psi} = \frac{1}{\sqrt{2}}$
$1 \oplus \psi$	(3) $\eta_{11} = \eta_{\psi 1} = \frac{1}{\sqrt{2}}$	(4) $\eta_{11} = \eta_{1\psi} = \eta_{\psi 1} = \eta_{\psi\psi} = \frac{1}{2}$ (5) $\eta_{11} = \eta_{\psi\psi} = \frac{1}{\sqrt{2}}$

Table 1. Solutions η for different algebra objects A_1 and A_2 in the \mathbb{Z}_2 fusion category. Algebras A_1 and A_2 both happen to be Frobenius algebras, respectively with multiplications $f_{ijk} = \delta_{ijk}$ and $g_{mnl} = \delta_{mnl}$ where $i, j, k \in A_1$ and $m, n, l \in A_2$.

correspond to nontrivial GDWs. To understand these GDWs, we can decompose these DW plaquette operators as

$$\begin{aligned}
B_p^{\text{DW}} &= \sum_{i \in A_1, j \in A_2} \eta_{ij}^2 v_i v_j B_p^{ij} \\
&= \sum_{i \in A_1, j \in A_2} \frac{1}{d_{A_1}} \frac{1}{d_{A_2}} \delta_{i \in A_1} \delta_{j \in A_2} v_i v_j B_p^{ij} \\
&= \sum_{i \in A_1, j \in A_2} \frac{1}{d_{A_1}} \frac{1}{d_{A_2}} (v_i B_{p_l}^i \otimes v_j B_{p_r}^j) \\
&= \left(\frac{1}{d_{A_1}} \sum_{i \in A_1} v_i B_{p_l}^i \right) \otimes \left(\frac{1}{d_{A_2}} \sum_{j \in A_2} v_j B_{p_r}^j \right) =: B_{p_l}^{\text{DW}} \otimes B_{p_r}^{\text{DW}},
\end{aligned} \tag{5.2}$$

In the third equality above, we rewrite B_p^{st} as $B_{p_l}^s \otimes B_{p_r}^t$, where p_l (p_r) labels the left (right) half of the plaquette p of the joining points. This decomposition is possible because the joining function can be expressed as $\eta_{ij} = \sqrt{d_{A_1}^{-1}} \sqrt{d_{A_2}^{-1}} \delta_{i \in A_1} \delta_{j \in A_2}$.

According to Ref. [8], a GB of the tailed LW model is specified by a Frobenius algebra object A of the model's input UFC. Such a GB consists of half plaquettes with plaquette operators defined as

$$B_p^{\text{GB}} = \frac{1}{d_A} \sum_{i \in A} v_i B_p^i, \tag{5.3}$$

which agrees with the form of the two half-plaquette operators $B_{p_l}^{\text{DW}}$ and $B_{p_r}^{\text{DW}}$ in the decomposition (5.2). This is natural because both A_1, A_2 in Eq. (5.2) are Frobenius algebras. As such, a DW plaquette operator B_p^{DW} is decomposed into the tensor product of two half-plaquette operators, as in Eq. (5.2).

In view of this decomposition, the GDW with the first DW plaquette operator $B_p^{\text{DW}_1}$ is understood as joining the two GBs of the toric code phases on both sides. Each GB is an m -boundary³, where anyon m condenses. Likewise, the GDW with the fourth DW plaquette operator $B_p^{\text{DW}_4}$ glues the two GBs of the toric code phases on both sides, each of which is an e -boundary, where anyon e condenses.

³Note that the convention of the $e(m)$ -boundary may differ from those in some literatures, where the $e(m)$ -boundary means $e(m)$ is confined at the GB.

The GDW with the second DW plaquette operator $B_p^{\text{DW}_2}$ joins an m -boundary of the \mathbb{Z}_2 LW model on the left and the e -boundary on the right. This GDW facilitates the transformation of a condensed anyon m on the left to a condensed anyon e on the right. In contrast, the GDW with the third DW plaquette operator $B_p^{\text{DW}_2}$ joins an e -boundary of the \mathbb{Z}_2 LW model on the left and the m -boundary on the right. These two GDWs can be distinguished by the following: When we weld the two composite systems vertically on top of each other, a junction would have to appear where the two GDWs are welded. The junction arises because we are welding an m -boundary with an e -boundary and vice versa[28].

Our model yields 5 GDWs within the \mathbb{Z}_2 LW model. Nevertheless, it is known that the \mathbb{Z}_2 LW model possesses another GDW, crossing which an anyon e (m) on one side becomes an anyon m (e) on the other side[4, 20, 26]. In our framework, this $e - m$ exchanging GDW separates the \mathbb{Z}_2 LW models with different input fusion categories of \mathbb{Z}_2 symmetry: one being $\mathcal{R}ep(\mathbb{Z}_2)$ and the other $\mathcal{V}ec(\mathbb{Z}_2)$.

5.2 $\mathcal{C}_1 = \mathcal{R}ep(\mathbb{Z}_2)$ and $\mathcal{C}_2 = \mathcal{V}ec(\mathbb{Z}_2)$: Realizing e-m exchange

Let us consider the GDW that separates a \mathbb{Z}_2 LW model with input $\mathcal{R}ep(\mathbb{Z}_2)$ and another \mathbb{Z}_2 model with input $\mathcal{V}ec(\mathbb{Z}_2)$. Note that \mathcal{C}_2 is not a subcategory of \mathcal{C}_1 . The two simple objects of $\mathcal{V}ec(\mathbb{Z}_2)$ are equivalent to the two irreducible A -bimodules N_0, N_1 of $\mathcal{R}ep(\mathbb{Z}_2)$, where A is the nontrivial Frobenius algebra object $1 \oplus \psi$ in $\mathcal{R}ep(\mathbb{Z}_2)$. More precisely, $N_0 = (1 \oplus \psi, P_{N_0})$ with trivial bimodule action tensors and $N_1 = (1 \oplus \psi, P_{N_1})$ with nontrivial bimodule action tensors given by (F.7) and (F.8) in Appendix.F.1.

The fusion rules of N_0 and N_1 are $\delta_{N_0 N_0 N_0} = \delta_{N_0 N_1 N_1} = 1$. The quantum dimensions for bimodules are $d_{N_0} = d_{N_1} = 1$. Moreover, 6j-symbols are given by $G_{N_k N_l N_n}^{N_i N_j N_m} = \delta_{N_i N_j N_m} \delta_{N_k N_l N_n} \delta_{N_j N_k N_n} \delta_{N_i N_n N_l}$. Table 2 records all possible triples (A_1, A_2, η) :

$A_1 \backslash A_2$	N_0	$N_0 \oplus N_1$
1	(2) $\eta_{1N_0} = 1$	(1) $\eta_{1N_0} = \eta_{1N_1} = \frac{1}{\sqrt{2}}$
$1 \oplus \psi$	(4) $\eta_{1N_0} = \eta_{\psi N_0} = \frac{1}{\sqrt{2}}$	(3) $\eta_{1N_0} = \eta_{1N_1} = \eta_{\psi N_0} = \eta_{\psi N_1} = \frac{1}{2}$
		(6) $\eta_{1N_0} = \eta_{\psi N_1} = \frac{1}{\sqrt{2}}$

Table 2. Solutions η for different algebra objects A_1 in $\mathcal{R}ep(\mathbb{Z}_2)$ and A_2 in $\mathcal{V}ec(\mathbb{Z}_2)$. Algebras A_1 in $\mathcal{R}ep(\mathbb{Z}_2)$ and A_2 in $\mathcal{V}ec(\mathbb{Z}_2)$ have multiplications $f_{ijk} = \delta_{ijk}$ and $g_{N_i N_j N_k} = \delta_{N_i N_j N_k}$, respectively, where $i, j, k \in A_1$ and $N_i, N_j, N_k \in A_2$.

We label the solutions in Table 2 according to the types of GDWs, as the first four solutions (1)-(4) in Table 2 have one-to-one correspondence with the first four solutions in

Table 1, as shown below:

$$\begin{aligned}
(1) \quad \eta_{11} = 1 & \quad \longleftrightarrow \quad \eta_{1N_0} = \eta_{1N_1} = 1/\sqrt{2} \\
(2) \quad \eta_{11} = \eta_{1\psi} = 1/\sqrt{2} & \quad \longleftrightarrow \quad \eta_{1N_0} = 1 \\
(3) \quad \eta_{11} = \eta_{\psi 1} = 1/\sqrt{2} & \quad \longleftrightarrow \quad \eta_{1N_0} = \eta_{1N_1} = \eta_{\psi N_0} = \eta_{\psi N_1} = 1/2 \\
(4) \quad \eta_{11} = \eta_{1\psi} = \eta_{\psi 1} = \eta_{\psi\psi} = 1/2 & \quad \longleftrightarrow \quad \eta_{1N_0} = \eta_{\psi N_0} = 1/\sqrt{2}
\end{aligned} \tag{5.4}$$

Here comes the question: What is the GDW corresponding to solution (6) in Table 2? Let us construct an interdomain ribbon operator that transports an anyon in the $\mathcal{R}ep(\mathbb{Z}_2)$ -model to another anyon in the $\mathcal{V}ec(\mathbb{Z}_2)$ -model. The interdomain ribbon operator must commute with the DW plaquette operators B_p^{DW} to ensure that it does not create any excitations in the GDW. Moreover, an observation from solution (6) is that the gluing function η always connects the DOF 1 (ψ) in the $\mathcal{R}ep(\mathbb{Z}_2)$ -model and the DOF N_0 (N_1) in the $\mathcal{V}ec(\mathbb{Z}_2)$ -model. Therefore, upon crossing the GDW, a $\mathcal{R}ep(\mathbb{Z}_2)$ -model anyon whose tail DOF is 1 (ψ) would become a $\mathcal{V}ec(\mathbb{Z}_2)$ -model anyon, whose tail DOF is N_0 (N_1).

According to the ribbon operators in the tailed LW model [25], the DOF of the tail for anyon e in the $\mathcal{R}ep(\mathbb{Z}_2)$ -model is ψ , while that for m in the $\mathcal{V}ec(\mathbb{Z}_2)$ -model is N_1 . We can construct the following operator, which can create e in the $\mathcal{R}ep(\mathbb{Z}_2)$ -model and m in the $\mathcal{V}ec(\mathbb{Z}_2)$ -model:

$$W_{E_1, E_2}^{e-m} \left| \begin{array}{c} E_1 \\ i_1 \\ i_3 \end{array} \right. \left. \begin{array}{c} a_1 \\ M_0 \\ p \\ a_2 \end{array} \right. \left. \begin{array}{c} b_1 \\ j_1 \\ j_2 \\ b_2 \end{array} \right. E_2 \rangle = \left| \begin{array}{c} \psi \\ i_1 \\ i_2 \\ i_3 \end{array} \right. \left. \begin{array}{c} z^e \\ \psi \\ M_0 \\ a_2 \end{array} \right. \left. \begin{array}{c} z^m \\ N_1 \\ j_1 \\ j_2 \\ j_3 \end{array} \right. \rangle. \tag{5.5}$$

Here, E_1, E_2 are the edges that intersect with the ribbon operator, whose DOFs are labeled by i_1, i_2 , respectively. The boxes labeled by z^e and z^m are half-braiding tensors correspond to e in the $\mathcal{R}ep(\mathbb{Z}_2)$ -model and m in the $\mathcal{V}ec(\mathbb{Z}_2)$ -model, and their data are given in Appendix B.1 and B.2. This ribbon operator commutes with the DW plaquette operator $B_p^{\text{DW}_6} = \frac{B_p^{1N_0} + B_p^{\psi N_1}}{2}$, which has been proven in Appendix D.2. Thus, this operator causes no excitation in the DW plaquette, and it is exactly the desired interdomain ribbon operator. Likewise, we can construct the DW-crossing ribbon operators W_{E_1, E_2}^{m-e} , W_{E_1, E_2}^{1-1} and $W_{E_1, E_2}^{\epsilon-\epsilon}$, all of which commute with $B_p^{\text{DW}_6}$. According to the proof in Appendix D.2, there are no other ribbon operators in the form of $W_{E_1, E_2}^{J_1-J_2}$. Therefore, anyons $1, \epsilon, e, m$ in the $\mathcal{R}ep(\mathbb{Z}_2)$ -model would become $1, \epsilon, m, e$ in the $\mathcal{V}ec(\mathbb{Z}_2)$ -model, respectively. So the GDW corresponding to Solution (6) is the e - m exchanging GDW.

Based on the analysis above, we can see that the GDW corresponding to Solution (6) realizes e - m exchange. Moreover, the results of $A_1 \overset{\eta}{\dashv} A_2$ -bimodules corresponding to Solution (6) and other four solutions in Table 2 are provided in Appendix F.1.

In summary, the \mathbb{Z}_2 toric code phase possesses six physically distinguishable GDWs:

- I. ($A_1 = 1, A_2 = 1, \eta_{11} = 1$) characterizes a GDW that is equivalent to joining two m -condensed boundaries of the toric code.

- II. ($A_1 = 1, A_2 = 1 \oplus \psi, \eta_{11} = \eta_{1\psi} = \frac{1}{2}$) characterizes a GDW that is equivalent to joining a left m -condensed boundary and a right e -condensed boundary of the toric code.
- III. ($A_1 = 1 \oplus \psi, A_2 = 1, \eta_{11} = \eta_{\psi 1} = \frac{1}{2}$) characterizes a GDW that is equivalent to joining a left e -condensed boundary and a right m -condensed boundary of the toric code.
- IV. ($A_1 = 1 \oplus \psi, A_2 = 1 \oplus \psi, \eta_{11} = \eta_{1\psi} = \eta_{\psi 1} = \eta_{\psi\psi} = \frac{1}{2}$) characterizes a GDW that is equivalent to joining two e -condensed boundaries of the toric code.
- V. ($A_1 = 1 \oplus \psi, A_2 = 1 \oplus \psi, \eta_{11} = \eta_{\psi\psi} = \frac{1}{\sqrt{2}}$) characterizes the trivial GDW in the toric code.
- VI. ($A_1 = 1 \oplus \psi, A_2 = N_0 \oplus N_1, \eta_{1N_0} = \eta_{\psi N_1} = \frac{1}{2}$) characterizes a GDW that realizes e - m exchange in the toric code.

6 GDWs in the doubled Ising phase

In this section, we consider GDWs in the doubled Ising phase. We find that our construction can derive all GDWs at the microscopic (input) level. However, from the classification at the macroscopic (output) level, some GDWs may lead to equivalent results.

The input fusion category of the doubled Ising LW model is the Ising fusion category, which has objects $\{1, \sigma, \psi\}$ with fusion rules $\psi \times \psi = 1, \sigma \times \sigma = 1 + \psi, \sigma \times \psi = \sigma$, so the quantum dimensions for each simple objects are $d_1 = d_\psi = 1, d_\sigma = \sqrt{2}$, and the fusion coefficients are

$$\delta_{111} = \delta_{1\sigma\sigma} = \delta_{1\psi\psi} = \delta_{\sigma\sigma\psi} = 1. \quad (6.1)$$

The nonvanishing $6j$ -symbols are

$$\begin{aligned} G_{111}^{111} &= 1, G_{\psi\psi\psi}^{111} = 1, G_{1\psi\psi}^{1\psi\psi} = 1, G_{\sigma\sigma\sigma}^{111} = \frac{1}{\sqrt[4]{2}}, \\ G_{1\sigma\sigma}^{1\sigma\sigma} &= \frac{1}{\sqrt{2}}, G_{\sigma\psi\psi}^{1\sigma\sigma} = \frac{1}{\sqrt[4]{2}}, G_{\psi\sigma\sigma}^{1\sigma\sigma} = \frac{1}{\sqrt{2}}, G_{\sigma\sigma\psi}^{\sigma\sigma\psi} = -\frac{1}{\sqrt{2}}. \end{aligned} \quad (6.2)$$

Solutions of η to Eq. (3.21) are listed below:

To understand which GDWs are characterized by the solutions in Table 3, we first note that the gluing functions in Solutions (1)-(4) satisfy the form: $\eta_{ab} = \sqrt{d_{A_1}^{-1}} \sqrt{d_{A_2}^{-1}} \delta_{a \in A_1} \delta_{b \in A_2}$. As a result, Solutions (1)-(4) characterize GDWs that result from gluing the two GBs of the doubled Ising. Moreover, $A = 1$ and $A = 1 \oplus \psi$ are Frobenius algebras that characterize the two Morita-equivalent GBs of the doubled Ising [8], so the four GDWs characterized by Solutions (1)-(4) are physically equivalent. The corresponding $A_1 \overset{\eta}{-} A_2$ -bimodules are given in Appendix. F.2.

$A_1 \backslash A_2$	1	$1 \oplus \psi$	$1 \oplus \psi \oplus \sigma$
1	(1) $\eta_{11} = 1$	(2) $\eta_{11} = \eta_{1\psi} = \frac{1}{\sqrt{2}}$	-
$1 \oplus \psi$	(3) $\eta_{11} = \eta_{\psi 1} = \frac{1}{\sqrt{2}}$	(4) $\eta_{11} = \eta_{1\psi} = \eta_{\psi 1} = \eta_{\psi\psi} = \frac{1}{2}$ (5) $\eta_{11} = \eta_{\psi\psi} = \frac{1}{\sqrt{2}}$	-
$1 \oplus \psi \oplus \sigma$	-	-	(6) $\eta_{11} = \eta_{\psi\psi} = \eta_{\sigma\sigma} = \frac{1}{2}$

Table 3. Solutions to η for different A_1 and A_2 in the LW Ising model. In this case, $f_{ijk} = \delta_{ijk}, g_{mnl} = \delta_{mnl}$ where $i, j, k \in A_1$ and $m, n, l \in A_2$.

Solution (5) characterizes a $\psi\bar{\psi}$ -condensation induced GDW. To illustrate this, we can construct an interdomain ribbon operator as follows:

$$W_{E_1, E_2}^{\psi\bar{\psi}-1\bar{1}} \left| \begin{array}{c|c|c} \text{red} & \text{white} & \text{blue} \\ \hline E_1 & M_0 & E_2 \\ \hline i_1 & p & j_1 \\ \hline i_3 & & j_3 \\ \hline i_2 & & j_2 \\ \hline a_2 & & b_2 \end{array} \right\rangle = \left| \begin{array}{c|c|c} \text{red} & \text{white} & \text{blue} \\ \hline i_1 & 1 & j_1 \\ \hline i_3 & z^{\psi\bar{\psi}} & z^{1\bar{1}} \\ \hline i_2 & & j_2 \\ \hline a_2 & & b_2 \end{array} \right\rangle. \quad (6.3)$$

This operator describes the process of $\psi\bar{\psi}$ -condensation across the GDW. As we will see in the next section, this condensation occurs between the doubled Ising phase and the toric code phase, thus Solution (5) describes a $(1+1)$ -dimensional defect formed by shrinking the toric code phase.

In conclusion, the six solutions in Table 3 lead to only three physically inequivalent GDWs in the doubled Ising topological phase:

- I. The first four solutions characterize a common GDW that is derived by gluing two Morita-equivalent GBs of the doubled Ising.
- II. ($A_1 = 1, A_2 = 1 \oplus \psi, \eta_{11} = \eta_{\psi\psi} = \frac{1}{\sqrt{2}}$) characterizes the $\psi\bar{\psi}$ -condensing GDW in the doubled Ising.
- III. ($A_1 = 1, A_2 = 1 \oplus \psi \oplus \sigma, \eta_{11} = \eta_{\psi\psi} = \eta_{\sigma\sigma} = \frac{1}{2}$) characterizes the trivial GDW in the doubled Ising.

7 GDWs between the doubled Ising and Toric code phases

Here, we compute GDWs separating the doubled Ising and the toric code. There are five solutions of the joining function η given different A_1 and A_2 , as listed in table 4.

The first four solutions labeled by (1)-(4) characterize GDWs that are obtained by gluing the GBs of the doubled Ising and toric code. Since the two GBs of the doubled Ising are equivalent [8], solutions (1) and (3) characterize the physically equivalent GDW

A_2	1	$1 \oplus \psi$
A_1		
1	(1) $\eta_{11} = 1$	(2) $\eta_{11} = \eta_{1\psi} = \frac{1}{\sqrt{2}}$
$1 \oplus \psi$	(3) $\eta_{11} = \eta_{\psi 1} = \frac{1}{\sqrt{2}}$	(4) $\eta_{11} = \eta_{1\psi} = \eta_{\psi 1} = \eta_{\psi\psi} = \frac{1}{2}$ (5) $\eta_{11} = \eta_{\psi\psi} = \frac{1}{\sqrt{2}}$

Table 4. Solutions to η for different A_1 and A_2 for the GDWs between Ising LW model and \mathbb{Z}_2 LW models. In this case, $f_{ijk} = \delta_{ijk}, g_{mnl} = \delta_{mnl}$ where $i, j, k \in A_1$ and $m, n, l \in A_2$, with A_1 and A_2 the Frobenius algebras for the Ising LW and the \mathbb{Z}_2 LW model, respectively.

that joins the GB of the doubled Ising and the m -boundary of the toric code. Similarly, Solutions (2) and (4) characterize the GDW that joins the GB of doubled Ising and the e -boundary of the toric code.

Solution (5) in Table 4 corresponds to a phase transition process. In this process, the right part of the Levin-Wen (LW) model, initially in the doubled Ising phase, undergoes $\psi\bar{\psi}$ -condensation and transitions into the toric code phase [6]. As a result, a GDW emerges at the interface between the toric code phase (on the right) and the remaining doubled Ising phase (on the left), which is precisely characterized by Solution (5).

In summary, the doubled Ising and \mathbb{Z}_2 topological phases can be separated by three physically distinct GDWs:

- I. $(A_1 = 1, A_2 = 1, \eta_{11} = 1)$ and $(A_1 = 1 \oplus \psi, A_2 = 1, \eta_{11} = \eta_{\psi 1} = \frac{1}{\sqrt{2}})$ characterize a GDW that is composed of the GB of the doubled Ising and the m -condensed boundary of the toric code.
- II. $(A_1 = 1, A_2 = 1 \oplus \psi, \eta_{11} = \eta_{1\psi} = \frac{1}{\sqrt{2}})$ and $(A_1 = 1 \oplus \psi, A_2 = 1 \oplus \psi, \eta_{11} = \eta_{1\psi} = \eta_{\psi 1} = \eta_{\psi\psi} = \frac{1}{2})$ correspond to a GDW that is composed of the GB of the doubled Ising and the e -condensed boundary of the toric code.
- III. $(A_1 = 1, A_2 = 1 \oplus \psi, \eta_{11} = \eta_{\psi\psi} = \frac{1}{\sqrt{2}})$ characterizes the $\psi\bar{\psi}$ -condensing GDW in the Ising LW model.

8 GDW-GB Correspondence

Seen in Fig. 4, our lattice is symmetric with respect to the middle line in the GDW, thus is convenient for investigating the folded phase on the lattice. After folding our model along the middle line, we find that the folded phase is described by the LW model with input UFC $\mathcal{C}_1^{\text{op}} \boxtimes \mathcal{C}_2$, and the GDW would become a boundary of the folded phase. Here, \boxtimes denotes the Deligne's tensor product, and $\mathcal{C}_2^{\text{op}}$ is the opposite category of \mathcal{C}_2 [2]. In this section, we show that each triple (A_1, A_2, η) characterizing a GDW would correspond to a Frobenius algebra in the input $\mathcal{C}_1^{\text{op}} \boxtimes \mathcal{C}_2$ for the folded phase.

We pair edges in A_1 to edges in A_2 of the GDW if they overlap after folding, and use these pairs to label the open edges (colored purple) at the boundary of the folded

phase. Now, we can show that the boundary derived by folding is a GB of the folded phase, which is characterized by a Frobenius algebra. The label set for the purple edges is $L_\eta = \{(i, j) | \eta_{ij} \neq 0, i \in A_1, j \in A_2\}$ defined in Eq. (3.3), which forms an algebra with the multiplication defined by:

$$\Omega_{(i',i)(j',j)(k',k)} \triangleq \bar{f}_{i'j'k'} g_{ijk} \Delta[\eta_{i'i} \eta_{j'j} \eta_{k'k}] = \bar{f}_{i'j'k'} g_{ijk}, \quad (8.1)$$

where $\bar{f}_{abc} = f_{bac}$. The second equality holds because $(i', i), (j', j), (k', k) \in L_\eta$. In the folded phase, the quantum dimension of an η -paired object is the product of the quantum dimensions of the two objects in the pair, i.e. $d_{(i',i)} = d_{i'} d_i$. We denote the algebra by $\bar{A}_1 \times_\eta A_2$, where \times_η represents the η -pairing between A_1 and A_2 . It is equipped with the following properties.

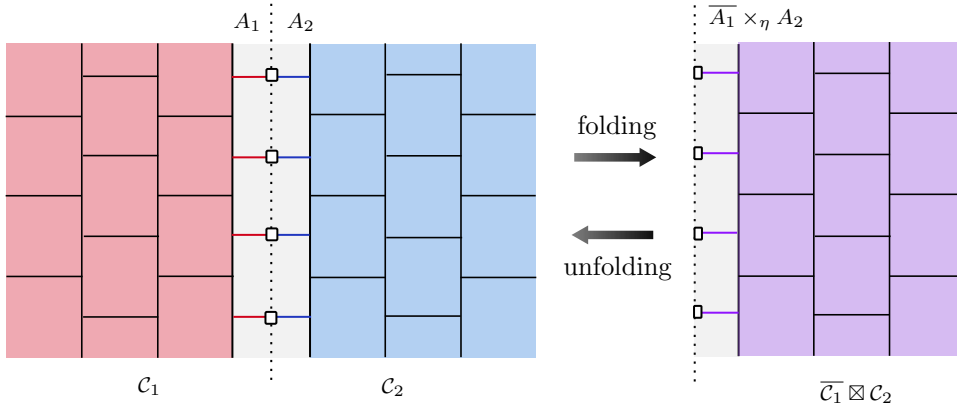


Figure 4. Fold the lattice for the ground states along the middle (dotted) line of the GDW. Then the DOFs at the gluing points in the GDW becomes those at the endpoints of tails (colored purple) in the GB. Since the DOFs at the endpoints of the tails are fixed by M_0 , we can omit it when discussing about the ground states.

- Unit condition: The unit object $(1, 1)$ in L_η is the pair of the units in L_{A_1} and L_{A_2} . Then, due to (3.2) and (8.1), the multiplication Ω should satisfy the following unit condition

$$\Omega_{(a,i)(a^*,i^*)(1,1)} = \Omega_{(a,i)(1,1)(a^*,i^*)} = \Omega_{(1,1)(a,i)(a^*,i^*)} = 1, \quad (8.2)$$

- Cyclic condition:

$$\Omega_{(a,i)(b,j)(c,k)} = \Omega_{(b,j)(c,k)(a,i)}. \quad (8.3)$$

- Associativity condition: According to the commutativity (3.21) for (A_1, A_2, η) , the algebra should also satisfy the following equation:

$$\mathcal{T} \left| \begin{array}{c} (i_1, j_1) \\ \uparrow \\ \text{---} \bullet \text{---} \bullet \text{---} \bullet \text{---} \\ \uparrow \quad \uparrow \\ (i_2, j_2) \quad (k_1, l_1) \\ (k_3, l_3) \end{array} \right\rangle = \left| \begin{array}{c} (i_1, j_1) \\ \uparrow \\ \text{---} \bullet \text{---} \bullet \text{---} \bullet \text{---} \\ \uparrow \quad \uparrow \\ (i_2, j_2) \quad (k_1, l_1) \\ (k_3, l_3) \end{array} \right\rangle, \quad (8.4)$$

which is explicitly the associativity condition for the boundary Frobenius algebra defined in [8].

- Strong condition: the projective condition (3.23) is the same as the strong condition of the Frobenius algebra:

$$\mathcal{T} \left(\sum_{(i',i),(j',j) \in L_\eta} (\eta_{i'i} \eta_{j'j})^2 \left| \begin{array}{c} (j',j) \\ \circlearrowleft \\ (i',i) \end{array} \right\rangle \right) = (\eta_{k'k})^2 \left| \begin{array}{c} (k',k) \\ \uparrow \\ (k',k) \end{array} \right\rangle. \quad (8.5)$$

Equations (8.2), (8.3), (8.4) and (8.5) together render the boundary algebra (L_A, Ω) a Frobenius algebra. Moreover, the Pachner moves in the GB of the folded model can be derived from the Pachner moves in the GDW:

$$\mathcal{T} \left| \begin{array}{c} (j',j) \\ \curvearrowright \\ (i',i) \end{array} \right\rangle = \sum_{(j',j),(i',i) \in L_\eta} \frac{u_{i'} u_i u_{j'} u_j}{u_{k'} u_k} \Omega_{(j'j)(i'i)(k'k)} \left| \begin{array}{c} (k',k) \\ \leftarrow \\ (k',k) \end{array} \right\rangle, \quad (8.6)$$

$$\mathcal{T} \left| \begin{array}{c} (k',k) \\ \leftarrow \\ (k',k) \end{array} \right\rangle = \frac{u_{i'} u_i u_{j'} u_j}{u_{k'} u_k} \Omega_{(j'j)(i'i)(k'k)} \left| \begin{array}{c} (j',j) \\ \curvearrowright \\ (i',i) \end{array} \right\rangle, \quad (8.7)$$

which align with the boundary Pachner moves derived in [8].

Example: Let us consider the 6 GDWs in the \mathbb{Z}_2 toric code phase. After folding, these GDWs become the GBs of a 2-layered toric code phase. Type 1-Type 6 GDWs would produce Frobenius algebras with the following multiplications, which have cyclic symmetry:

- DW₁: $L_\eta = \{(1, 1)\}$

$$\Omega_{(1,1)(1,1)(1,1)} = 1 \quad (8.8)$$

- DW₂: $L_\eta = \{(1, 1), (1, \psi)\}$

$$\Omega_{(1,1)(1,1)(1,1)} = \Omega_{(1,1)(1,\psi)(1,\psi)} = 1 \quad (8.9)$$

- DW₃: $L_\eta = \{(1, 1), (\psi, 1)\}$

$$\Omega_{(1,1)(1,1)(1,1)} = \Omega_{(\psi,1)(\psi,1)(1,1)} = 1 \quad (8.10)$$

- DW₄: $L_\eta = \{(1, 1), (1, \psi), (\psi, 1), (\psi, \psi)\}$

$$\begin{aligned} \Omega_{(1,1)(1,1)(1,1)} &= \Omega_{(1,1)(1,\psi)(1,\psi)} = \Omega_{(1,1)(\psi,1)(\psi,1)} = 1, \\ \Omega_{(1,1)(\psi,\psi)(\psi,\psi)} &= \Omega_{(1,\psi)(\psi,\psi)(\psi,1)} = \Omega_{(1,\psi)(\psi,1)(\psi,\psi)} = 1. \end{aligned} \quad (8.11)$$

- DW₅: $L_\eta = \{(1, 1), (\psi, \psi)\}$

$$\Omega_{(1,1)(1,1)(1,1)} = \Omega_{(1,1)(\psi,\psi)(\psi,\psi)} = 1. \quad (8.12)$$

- DW₆: For $e - m$ exchanging GDW, we have transformed the basis of the right model. So the label set of algebra $\bar{A}_1 \times A_2$ transforms from $L_\eta = \{(1, M_0), (\psi, M_1)\}$ to $L_\eta = \{(1, 1), (1, \psi), (\psi, 1), (\psi, \psi)\}$. Eq. (8.1) is modified as follows:

$$\Omega_{(a_1, b_1), (a_2, b_2), (a_3, b_3)} = \sum_{M_i, M_j, M_k} \bar{f}_{a_1 a_2 a_3} \tilde{g}_{b_1 b_2 b_3}^{M_i M_j M_k} \Delta(\eta_{a_1 M_i} \eta_{a_2 M_j} \eta_{a_3 M_k}), \quad (8.13)$$

where $\tilde{g}_{b_1 b_2 b_3}^{M_i M_j M_k}$ are the expansion coefficients for the multiplication of A_2 , which is given in Appendix F.1. Then,

$$\begin{aligned} \Omega_{(1,1)(1,1)(1,1)} &= \Omega_{(1,1)(1,\psi)(1,\psi)} = 1, \\ \Omega_{(1,1)(\psi,1)(\psi,1)} &= 1, \Omega_{(1,1)(\psi,\psi)(\psi,\psi)} = 1, \\ \Omega_{(1,\psi)(\psi,\psi)(\psi,1)} &= i, \Omega_{(1,\psi)(\psi,1)(\psi,\psi)} = -i. \end{aligned} \quad (8.14)$$

9 Conclusions and Outlook

In this paper, we have developed a novel framework for constructing GDWs within the LW model. By sewing two LW models along their open sides using algebra objects from their respective input UFCs, we provide a systematic approach that results in exactly solvable, gapped Hamiltonians to describe all GDWs between the two models. The construction introduces new DOFs at the joining point, which are captured by $A_1 \overset{\eta}{\bowtie} A_2$ -bimodules. This approach offers a unified description of GDWs, including those that involve anyon condensation and e - m exchange.

Our framework for constructing GDWs is fully compatible with the folding trick. Specifically, after folding the lattice along the GDW, the algebra $\bar{A}_1 \times_{\eta} A_2$ emerges as the Frobenius algebra that characterizes the GBs of the folded model with input $\bar{\mathcal{C}}_1 \boxtimes \mathcal{C}_2$, where \times_{η} denotes the η -pairing between A_1 and A_2 . This connection between GDWs and GBs highlights the robustness and topological nature of the construction.

While our approach provides a novel and general method for constructing GDWs, there are several avenues for future work along this line:

- (1) Our method is able to classify GDWs by their Hamiltonians, which is at the level of input UFC. Nevertheless, to derive all physically inequivalent GDWs, we need further analyses, and those analyses are not systematic enough. We also state that two GDWs are physically equivalent if they are obtained by gluing two GBs which are Morita equivalent respectively for each side. In fact, we mix the concept of Morita equivalence in Mathematics and the concept of physical equivalence. It remains further investigation.
- (2) The fusion of GDWs and the construction of junctions between them, which are codimension-2 defects, is crucial for the completeness of the extended TQFT. For example, consider a GDW that separates the doubled Ising model and the toric code, and another GDW that realizes e - m exchange in the toric code. When these two GDWs fuse, a junction appears where they meet. A detailed understanding of how to construct such junctions and the corresponding excitation spectrum at the junctions is a key open problem. Developing a framework to describe these junctions will provide a more complete picture of topological defects.

In conclusion, our work provides a systematic and concrete approach to studying GDWs in topologically ordered phases, offering new insights into their role in defect theories. Future research will aim to extend this framework to higher dimensions and explore the full range of physical phenomena that can emerge from the fusion and interaction of these GDWs.

Acknowledgments

YC thank Yingcheng Li, Hongyu Wang and Zhihao Zhang for helpful discussions. YW is supported by NSFC Grant No. 12475001, Shanghai Municipal Science and Technology Major Project No. 2019SHZDZX01, the Science and Technology Commission of Shanghai Municipality (Grant No. 24LZ1400100), and the Innovation Program for Quantum Science

and Technology ZD0220240101 (PZ). YW is grateful for the hospitality of the Perimeter Institute during his visit, where part of this work is done. This research was supported in part by the Perimeter Institute for Theoretical Physics. Research at Perimeter Institute is supported by the Government of Canada through the Department of Innovation, Science and Economic Development and by the Province of Ontario through the Ministry of Research, Innovation and Science.

A Review of the LW model

A.1 The original LW model

The LW model, also called the string net model [29], is described by an input unitary fusion category \mathcal{C} with data $\{d_j, N_{ij}^k, G_{ijk}^{mnl}\}$. It is defined on a two-dimensional trivalent lattice with oriented edges denoted by simple objects of the input UFC \mathcal{C} . Every object has its dual object, which can be obtained by reversing the orientation of an edge. Denote the label set of all simple objects in \mathcal{C} by L . The fusion rule of strings is defined by $i \otimes j = \oplus_k N_{ij}^k k$, where $N : L \times L \times L \rightarrow \mathbb{N}$. The fusion coefficient N_{ij}^k should satisfy the following conditions that for any $a, b, c, d \in L$,

$$N_{0a}^b = N_{a0}^b = \delta_{ab}, \quad (\text{A.1})$$

$$N_{ab}^0 = \delta_{ab^*}, \quad (\text{A.2})$$

$$\sum_{x \in L} N_{ab}^x N_{xc}^d = \sum_{x \in L} N_{ax}^d N_{cb}^x. \quad (\text{A.3})$$

Every three edges meeting at a same vertex should obey the fusion rule in a proper lattice configuration. When the category is multiplicity-free, $N_{ij}^k = \delta_{ijk^*}$.

The quantum dimension d_j of string type j is the one-dimensional representation of the fusion rule, which satisfies:

$$d_i d_j = \sum_k N_{ij}^k d_k. \quad (\text{A.4})$$

Finally, the unitary symmetric tetrahedral $6j$ symbols are denoted by G_{ijk}^{lmn} . They satisfy the following conditions:

$$\text{tetrahedral symmetry: } G_{klm}^{ijn} = G_{nk^*l^*}^{mij} = G_{ijl^*n^*}^{k^*lm} = \alpha_m \alpha_n G_{l^*k^*n^*}^{j^*i^*m^*}, \quad (\text{A.5})$$

$$\text{associativity: } \sum_n d_n G_{kp^*n}^{mlq} G_{mns^*}^{jip} G_{lkr^*}^{js^*n} = G_{q^*kr^*}^{jip} G_{mns^*}^{riq^*}, \quad (\text{A.6})$$

$$\text{orthogonality: } \sum_n d_n G_{kp^*n}^{mlq} G_{pk^*n}^{d^*m^*j^*} = \frac{\delta_{iq}}{d_i} \delta_{mlq} \delta_{k^*ip}. \quad (\text{A.7})$$

The Hamiltonian of the bulk LW model is the sum of all vertex operators A_v and plaquette operators B_p , which are commutative projectors:

$$H = - \sum_v A_v - \sum_p B_p. \quad (\text{A.8})$$

The vertex operator A_v is to check if the trivalent vertex v satisfies the fusion rule. It indicates a charge excitation at vertex v if $\delta_{ijk^*} = 0$, which is a discrete version of the Gauss law for electric fields.

$$A_v \left| \begin{array}{c} k \\ \uparrow \\ i \swarrow \quad \searrow j \end{array} \right\rangle = \delta_{ijk^*} \left| \begin{array}{c} k \\ \uparrow \\ i \swarrow \quad \searrow j \end{array} \right\rangle. \quad (\text{A.9})$$

The B_p is a plaquette operator defined by the following equation, which means inserting string loops of all types into plaquette p and fusing them with the boundary of the plaquette.

$$B_p = \frac{1}{D} \sum_s d_s B_p^s, \quad (\text{A.10})$$

where D is the total quantum dimension $D = \sum_{s \in \text{Ob}(\mathcal{C})} d_s^2$ and

$$B_p^s \left| \begin{array}{c} k_1 \quad i'_6 \quad k_6 \\ \leftarrow k_2 \quad \leftarrow i'_1 \quad \leftarrow i'_2 \quad \leftarrow i'_3 \quad \leftarrow k_3 \\ \leftarrow i'_4 \quad \leftarrow i'_5 \quad \leftarrow k_4 \quad \leftarrow k_5 \end{array} \right\rangle = \left| \begin{array}{c} k_1 \quad i'_6 \quad k_6 \\ \leftarrow k_2 \quad \leftarrow i'_1 \quad \leftarrow i'_2 \quad \leftarrow i'_3 \quad \leftarrow k_3 \\ \leftarrow i'_4 \quad \leftarrow i'_5 \quad \leftarrow k_4 \quad \leftarrow k_5 \end{array} \right\rangle = \sum_{i_1, i_2, i_3, i_4, i_5, i_6, s \in \mathcal{C}} G_{s^* i_6 i_1}^{k_1 i'_1 i'_6} G_{i_2 s i_1}^{i'_1 k_2 i'_2} \quad (\text{A.11})$$

$$G_{i_3^* s i_2}^{i'_2 k_3 i'_3} G_{s^* i_3 i_4}^{k_4 i'_4 i'_3} G_{s^* i_4 i_5}^{k_5 i'_5 i'_4} G_{i_6 s i_5}^{i'_5 k_6 i'_6} v_{i_1} v_{i_2} v_{i_3} v_{i_4} v_{i_5} v_{i_6} v_{i'_1} v_{i'_2} v_{i'_3} v_{i'_4} v_{i'_5} v_{i'_6} \left| \begin{array}{c} k_1 \quad i_6 \quad k_6 \\ \leftarrow i_1 \quad \leftarrow i_2 \quad \leftarrow i_3 \quad \leftarrow i_4 \\ \leftarrow i_5 \quad \leftarrow i_6 \quad \leftarrow k_5 \end{array} \right\rangle \quad (\text{A.12})$$

A.2 The tailed LW model with enlarged Hilbert space

The tailed LW model is an extension of the original LW model, and is useful for investigating quasiparticle excitations. The Hilbert space of the conventional LW model is enlarged to hold charge excitations. As shown in Fig. 5, we associate a tail to each vertex in the conventional LW model and the DOFs of those tails take value in \mathcal{C} . To distinguish the vertices emerging after introducing tails from the vertices in the conventional model, we call the original vertices the primary vertices, and call the new vertex joining one tail and two bulk edges the secondary vertex. Then, we find the tails can present the internal charge DOFs of quasiparticle excitations to every primary vertex [25]. Now, the Hilbert space is spanned by configurations of all the edge DOFs on the lattice, including the tails. At each trivalent vertex for the basis states in the Hilbert space, the fusion rules should always be satisfied.

The Hamiltonian of the tailed LW model is also the sum of all vertex operators and plaquette operators:

$$H = - \sum_v A_v - \sum_p B_p. \quad (\text{A.13})$$

The vertex operator defined for each primary vertex is modified as follows:

$$\mathcal{A}_v \left| \begin{array}{c} k_2 \uparrow \\ k_1 \uparrow \rightarrow q \\ i \rightarrow \quad j \rightarrow \end{array} \right\rangle = \delta_{q,1} \left| \begin{array}{c} k_2 \uparrow \\ k_1 \uparrow \rightarrow q \\ i \rightarrow \quad j \rightarrow \end{array} \right\rangle. \quad (\text{A.14})$$

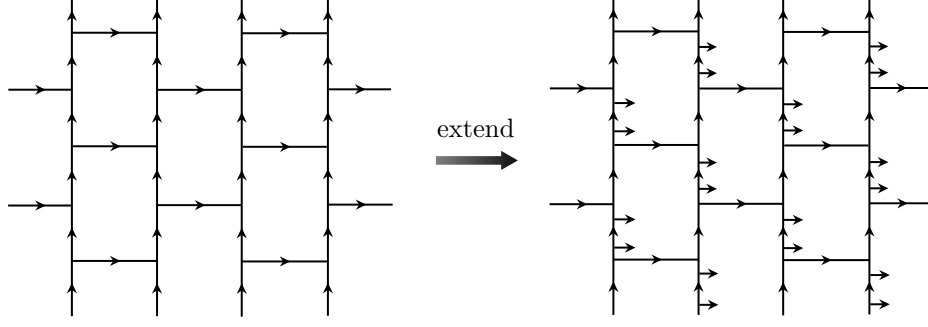


Figure 5. The extended LW model by enlarging the Hilbert space

Since the fusion rules are always satisfied, we have $\delta_{ijk_1} = 1, \delta_{k_1 k_2 q} = 1$ for the basis state above. One can see that the action of the vertex operators is to project a state to the ground state without any excitations at vertices. The plaquette operator is

$$B_p = \frac{1}{D} \sum_s d_s B_p^s, \quad (\text{A.15})$$

with

$$\begin{aligned}
& B_p^s \left| \begin{array}{c} k_1 \\ i'_1 \\ j'_1 \\ k_2 \\ i'_2 \\ i'_3 \\ k_3 \end{array} \right. \left. \begin{array}{c} i'_8 \\ k_6 \\ i'_7 \\ k_5 \\ i'_6 \\ q_3 \\ j'_2 \\ q_4 \\ i'_5 \\ k_4 \end{array} \right\rangle = \delta_{q_1,1} \delta_{q_2,1} \sum_{j_1, j_2, i_3, i_4, i_5, i_6, i_7, i_8} G_{k_1 j_1 i'_1}^{s* i_8' i_8} G_{k_2 i_3 i'_3}^{s* j_1' j_1} G_{k_3 i_4 i'_4}^{s* i_3' i_3} \\
& \times G_{k_4 i_5 i'_5}^{s* i_4' i_4} G_{q_4 j_2 i'_2}^{s* i_5' i_5} G_{q_3 i_6 i'_6}^{s* j_2' j_2} G_{k_5 i_6 i'_6}^{s* i_6' i_6} G_{k_6 i_7 i'_7}^{s* i_7' i_7} v_{j_1} v_{j_1'} v_{j_2} v_{j_2'} v_{i_3} v_{i_3'} v_{i_4} v_{i_4'} v_{i_5} v_{i_5'} v_{i_6} v_{i_6'} \\
& \times v_{i_7} v_{i_7'} v_{i_8} v_{i_8'} \left| \begin{array}{c} k_1 \\ j_1 \\ \dots 1 \\ j_1 \\ \dots 1 \\ j_1 \\ i_3 \\ k_3 \end{array} \right. \left. \begin{array}{c} i_8 \\ k_6 \\ i_7 \\ k_5 \\ i_6 \\ q_3 \\ j_2 \\ q_4 \\ i_5 \\ k_4 \end{array} \right\rangle. \quad (\text{A.16})
\end{aligned}$$

The plaquette operator in the extended Hamiltonian projects out the states with non-trivial tails in that plaquette. Moreover, the ground states are the eigenvectors of all plaquette operators and vertex operators that correspond to the eigenvalues +1. one can observe that the ground states of the tailed LW model are exactly the same as those of the traditional LW model.

B Ribbon operators in the bulk

The ribbon operators to create elementary excitations are characterized by the minimal solutions of half-braiding tensors, which capture the effects of a quasiparticle moving across an edge. These tensors encode essential information such as changes in the internal charges of the quasiparticle and the phase factor associated with the braiding process [7, 25]. The following equation illustrates a ribbon operator acting on the neighboring plaquettes with a shared edge E and creates a pair of dyons $(J, p), (J, q)$ at its ends:

$$W_E^{J;pq} \left| \begin{array}{c} i \nearrow \\ \\ \\ \\ m \searrow \end{array} \right\rangle = \sum_{l'} \frac{v_{l'}}{v_l} z_{p'l'ql}^J \left| \begin{array}{c} i \nearrow \\ \\ \\ \\ m \searrow \end{array} \right\rangle = \left| \begin{array}{c} i \nearrow \\ \\ \\ \\ m \searrow \end{array} \right\rangle, \quad (\text{B.1})$$

where z^J is the half-braiding tensor of the quasiparticle (dyon species) J . The half-braiding tensor satisfies the following naturality condition.

$$\left| \begin{array}{c} k \nearrow \\ \\ \\ \\ j \searrow \end{array} \right\rangle = \left| \begin{array}{c} k \nearrow \\ \\ \\ \\ j \searrow \end{array} \right\rangle. \quad (\text{B.2})$$

It is formulated as

$$\sum_{k', i', j', j_1} d_{k'} d_{i'} z_{pk'qk}^J z_{q^* i' r i}^J G_{j i j'}^{k' p k} G_{q k i'}^{j' i k'} G_{k j' j_1}^{r i i'} v_{j_1} = \sum_{j'} \frac{1}{v_j} z_{p j' r j}^J. \quad (\text{B.3})$$

The measuring operators for a dyon species J is defined as

$$\Pi_J = \sum_q \Pi_q^J, \quad \Pi_q^J = \sum_{s,t} \Pi_{qst}^J B_{qsqt}, \quad (\text{B.4})$$

where q is the internal charge of J and

$$B_{qsqt} \left| \begin{array}{c} \\ \\ \\ \\ \end{array} \right\rangle = \left| \begin{array}{c} \\ \\ \\ \\ \end{array} \right\rangle. \quad (\text{B.5})$$

When $J = J_0$ is a trivial excitation of zero charge, the corresponding measuring operator is $\Pi_{J_0} = \sum_s \Pi_{1s1s}^{J_0} B_{1s1s}$. Here, the coefficient $\Pi_{1s1s}^{J_0} = d_s/D$ and B_{1s1s} is the same as the plaquette operator B_p in the traditional LW model. Also, not only Π_q^J for each (J, q) is a projector, but their sum Π_J is a projector because of the orthogonality condition

$\Pi_q^J \cdot \Pi_{q'}^J = \delta_{qq'} \Pi_q^J$. Since Π_J is spanned by the basis B_{qsqt} , we can compute the following equation

$$\sum_{m,n,s,t,l,r} \Pi_{qns}^J \Pi_{qmt}^J \left| \begin{array}{c} \text{Diagram 1} \\ \text{Diagram 2} \end{array} \right\rangle = \sum_{l,r} \Pi_{qlr}^J \left| \begin{array}{c} \text{Diagram 3} \end{array} \right\rangle, \quad (\text{B.6})$$

and then derive the orthogonality condition for Π_{qst}^J :

$$d_l d_r \sum_{m,n,s,t} \Pi_{qns}^J \Pi_{qmt}^J G_{ns^*r}^{m^*tq^*} G_{q^*n^*l}^{m^*rs^*} G_{ln^*r}^{t^*qm} = \Pi_{qlr}^J. \quad (\text{B.7})$$

Also from Eq. B.6, we can see these measuring operators form a tube algebra and we denote it by \mathcal{A} . Since each Π^J correspond to a quasiparticle J , the states with elementary excitations are characterized by irreducible representations of \mathcal{A} . Additionally, Π_q^J living in a subspace spanned by B_{qsqt} with fixed charge q can form a subalgebra \mathcal{A}_q . Dyons are identified by operators Π_q^J , each of which corresponding to the minimal solutions of Eq. B.7. The minimal solution for means that if $\Pi_q^J = (\Pi_q^J)_1 + (\Pi_q^J)_2$, then either $(\Pi_q^J)_1$ or $(\Pi_q^J)_2$ is zero.

Since the state $W^{J;pq} \left| \psi_{gs} \right\rangle$ with dyon (J, q) excitations is the $+1$ eigenstate of Π_q^J , the coefficients Π_{qst}^J shows close relation with the half-braiding tensors z_{qsqt}^J :

$$\frac{\Pi_{qst}^J}{\Pi_{q1q}^J} = \frac{d_s d_t}{d_q} z_{qsqt}^J. \quad (\text{B.8})$$

We present several examples in the following sections.

B.1 The LW \mathbb{Z}_2 with input $\mathcal{Rep}(\mathbb{Z}_2)$

There are four dyon species $1, e, m, \varepsilon$ in the \mathbb{Z}_2 LW model, and the minimal solutions have a one-to-one correspondence with them as follows:

$$1 \quad z_{1111} = 1, \quad z_{1\psi 1\psi} = 1 \quad (\text{B.9})$$

$$e \quad z_{\psi\psi\psi 1} = 1, \quad z_{\psi 1\psi\psi} = 1 \quad (\text{B.10})$$

$$m \quad z_{1111} = 1, \quad z_{1\psi 1\psi} = -1 \quad (\text{B.11})$$

$$\varepsilon \quad z_{\psi 1\psi\psi} = -1, \quad z_{\psi\psi\psi 1} = 1 \quad (\text{B.12})$$

B.2 The LW \mathbb{Z}_2 with input $\mathcal{V}ec(\mathbb{Z}_2)$

As mentioned in Section 5.2, $\mathcal{V}ec(\mathbb{Z}_2)$ has two simple objects represented by the irreducible A - A -bimodules N_0 and N_1 of $\mathcal{R}ep(\mathbb{Z}_2)$, where $A = 1 \oplus \psi$ the nontrivial Frobenius algebra in $\mathcal{R}ep(\mathbb{Z}_2)$. The minimal solutions to Eq. (B.3) for $\mathcal{V}ec(\mathbb{Z}_2)$ are given below:

$$1 \quad z_{N_0 N_0 N_0 N_0} = 1, \quad z_{N_0 N_1 N_0 N_1} = 1 \quad (\text{B.13})$$

$$m \quad z_{N_1 N_1 N_1 N_0} = 1, \quad z_{N_1 N_0 N_1 N_1} = 1 \quad (\text{B.14})$$

$$e \quad z_{N_0 N_0 N_0 N_0} = 1, \quad z_{N_0 N_1 N_0 N_1} = -1 \quad (\text{B.15})$$

$$\varepsilon \quad z_{N_1 N_0 N_1 N_1} = -1, \quad z_{N_1 N_1 N_1 N_0} = 1 \quad (\text{B.16})$$

The categories $\mathcal{V}ec(\mathbb{Z}_2)$ and $\mathcal{R}ep(\mathbb{Z}_2)$ are equivalent. One can observe that replacing N_0, N_1 of $\mathcal{V}ec(\mathbb{Z}_2)$ with $1, \psi$, respectively would reproduce the fusion rules, 6j-symbols of $\mathcal{R}ep(\mathbb{Z}_2)$. As a result, solutions to Eq. (B.2) of half-braiding tensors in the basis $\{N_0, N_1\}$ have one-to-one correspondence with those in the basis $\{1, \psi\}$. Nevertheless, the correspondence between the minimal solutions of half-braiding tensors and the species of quasiparticles in the $\mathcal{V}ec(\mathbb{Z}_2)$ -model differs from that in the $\mathcal{R}ep(\mathbb{Z}_2)$ -model: e and m in Eq. (B.10) and (B.11) are exchanged in Eq. (B.15) and (B.14).

The exchange of e and m can be understood through the symmetry transformations. Any basis state of the $\mathcal{V}ec(\mathbb{Z}_2)$ -model transforms into a basis state of the $\mathcal{R}ep(\mathbb{Z}_2)$ as follows: (1) Each edge labeled by N_0 or N_1 is mapped to $\{1, \psi\}$; (2) Each vertex in the bulk satisfies the following expansion [30]:

$$\begin{array}{c} \text{---} M_i \\ \text{---} v \text{---} \\ \text{---} M_k \text{---} \\ \text{---} M_j \end{array} = \sum_{a \in L_{N_0}, b \in L_{N_0}, c \in L_{N_0}} \mathcal{V}_{abc}^{N_i N_i N_k} \begin{array}{c} \text{---} a \\ \text{---} v \text{---} \\ \text{---} c \text{---} \\ \text{---} b \end{array}, \quad (\text{B.17})$$

where the expansion coefficients are

$$\begin{aligned} \mathcal{V}_{111}^{N_0 N_0 N_0} &= \mathcal{V}_{1\psi\psi}^{N_0 N_0 N_0} = \mathcal{V}_{\psi 1\psi}^{N_0 N_0 N_0} = \mathcal{V}_{\psi\psi 1}^{N_0 N_0 N_0} = 1 \\ \mathcal{V}_{111}^{N_0 N_1 N_1} &= \mathcal{V}_{1\psi\psi}^{N_0 N_1 N_1} = 1, \quad \mathcal{V}_{\psi 1\psi}^{N_0 N_1 N_1} = i, \quad \mathcal{V}_{\psi\psi 1}^{N_0 N_1 N_1} = -i. \end{aligned} \quad (\text{B.18})$$

Using the basis transformation in Eq. (B.17), one can show that, for instance, the half-braiding tensors for m (e) in (B.14) ((B.15)) will transform into those in (B.11) ((B.10)).

B.3 The Ising LW

The minimal solutions to the half-braiding tensors of doubled Ising are listed below, and they are associated with the 9 dyon species of the Ising LW. Here we set $\omega = \exp\{\pi i/8\} = (-1)^{1/8}$.

$$1\bar{1} \quad z_{1111} = 1, \quad z_{1\psi 1\psi} = 1, \quad z_{1\sigma 1\sigma} = 1 \quad (\text{B.19})$$

$$\psi\bar{\psi} \quad z_{1111} = 1, \quad z_{1\psi 1\psi} = 1, \quad z_{1\sigma 1\sigma} = -1 \quad (\text{B.20})$$

$$\sigma\bar{\sigma} \quad \begin{aligned} z_{1111} &= 1, & z_{1\psi 1\psi} &= -1, \\ z_{\psi 1\psi\psi} &= 1, & z_{\psi\psi\psi 1} &= 1, \\ z_{1\sigma\psi\sigma} &= \pm 1, & z_{\psi\sigma 1\sigma} &= \pm 1. \end{aligned} \quad (\text{B.21})$$

$$\psi\bar{1} \quad z_{\psi 1\psi\psi} = -1, \quad z_{\psi\psi\psi 1} = 1, \quad z_{\psi\sigma\psi\sigma} = i. \quad (\text{B.22})$$

$$1\bar{\psi} \quad z_{\psi 1\psi\psi} = -1, \quad z_{\psi\psi\psi 1} = 1, \quad z_{\psi\sigma\psi\sigma} = -i. \quad (\text{B.23})$$

$$\sigma\bar{1} \quad z_{\sigma 1\sigma\sigma} = \omega, \quad z_{\sigma\sigma\sigma 1} = 1, \quad z_{\sigma\sigma\sigma\psi} = i, \quad z_{\sigma\psi\sigma\sigma} = -i\omega. \quad (\text{B.24})$$

$$1\bar{\sigma} \quad z_{\sigma 1\sigma\sigma} = \omega^*, \quad z_{\sigma\sigma\sigma 1} = 1, \quad z_{\sigma\sigma\sigma\psi} = -i, \quad z_{\sigma\psi\sigma\sigma} = i\omega^*. \quad (\text{B.25})$$

$$\sigma\bar{\psi} \quad z_{\sigma 1\sigma\sigma} = -\omega, \quad z_{\sigma\sigma\sigma 1} = 1, \quad z_{\sigma\sigma\sigma\psi} = i, \quad z_{\sigma\psi\sigma\sigma} = i\omega. \quad (\text{B.26})$$

$$\psi\bar{\sigma} \quad z_{\sigma 1\sigma\sigma} = -\omega^*, \quad z_{\sigma\sigma\sigma 1} = 1, \quad z_{\sigma\sigma\sigma\psi} = -i, \quad z_{\sigma\psi\sigma\sigma} = -i\omega^*. \quad (\text{B.27})$$

C Exactly solvable conditions to determine B_p^{DW}

C.1 Projective condition

The plaquette operator B_p^{DW} requires to be projective, i.e. $(B_p^{\text{DW}})^2 \stackrel{!}{=} B_p^{\text{DW}}$, which is computed graphically as follows. Without loss of generality, we can consider the DW plaquette operator B_p^{DW} acting on a basis state with trivial $A_1 \overset{n}{\perp} A_2$ -bimodules.

$$\begin{aligned}
(B_p^{\text{DW}})^2 \left| \begin{array}{c} \text{---} \\ \text{---} \\ \text{---} \\ \text{---} \end{array} \right\rangle &= \sum_{i',j' \in A_1, i,j \in A_2} v_{i'} v_i v_{j'} v_j (\eta_{i' i} \eta_{j' j})^2 \left| \begin{array}{c} \text{---} \\ \text{---} \\ \text{---} \\ \text{---} \end{array} \right\rangle \\
&= \sum_{i',j' \in A_1, i,j \in A_2} v_{i'} v_i v_{j'} v_j (\eta_{i' i} \eta_{j' j})^2 \sum_{k' \in A_1, k \in A_2} G_{j' i' k'}^{i i' * 1} v_{k'} G_{j j' k}^{i * 1} v_k \left| \begin{array}{c} \text{---} \\ \text{---} \\ \text{---} \\ \text{---} \end{array} \right\rangle \\
&= \sum_{i',j',k' \in A_1, i,j,k \in A_2} v_{k'} v_k (\eta_{i' i} \eta_{j' j})^2 \delta_{i' j' k'} \delta_{i j k} \left| \begin{array}{c} \text{---} \\ \text{---} \\ \text{---} \\ \text{---} \end{array} \right\rangle \\
&\stackrel{(3.19)}{=} \sum_{i',j',k' \in A_1, i,j,k \in A_2} v_{i'} v_{j'} v_i v_j (\eta_{i' i} \eta_{j' j})^2 \delta_{i' j' k'} \delta_{i j k} f_{i' j' k'}^{i i' * j' k'} f_{j j' k}^{i * j' k} g_{j i k} g_{i j k} \left| \begin{array}{c} \text{---} \\ \text{---} \\ \text{---} \\ \text{---} \end{array} \right\rangle \\
&\stackrel{!}{=} \sum_{k' \in A_1, k \in A_2} v_{k'} v_k (\eta_{k' k})^2 \delta_{i' j' k'} \delta_{i j k} \left| \begin{array}{c} \text{---} \\ \text{---} \\ \text{---} \\ \text{---} \end{array} \right\rangle = B_p^{\text{DW}} \left| \begin{array}{c} \text{---} \\ \text{---} \\ \text{---} \\ \text{---} \end{array} \right\rangle.
\end{aligned}$$

Therefore, the projective condition is given by

$$\sum_{\substack{i',j' \in \tilde{A} \\ i,j \in A}} \sum_{\eta_{k' k} \neq 0} \delta_{i' j' k'} \delta_{i j k} \frac{v_{i'} v_{j'} v_i v_j}{v_k v_{k'}} f_{i' j' k'}^{i i' * j' k'} f_{j j' k}^{i * j' k} g_{j i k} g_{i j k} (\eta_{j' j} \eta_{i' i})^2 = (\eta_{k' k})^2. \quad (\text{C.1})$$

It can be represented graphically as

$$\mathcal{T}\left(\sum_{i',j' \in A_1, i, j \in A_2} (\eta_{i'i} \eta_{j'j})^2 \left| \begin{array}{c} \text{---} \square \text{---} \\ \text{---} \square \text{---} \\ \text{---} \square \text{---} \end{array} \right. \right\rangle = \Delta[\eta_{j'j} \eta_{i'i} \eta_{k'k}] \cdot (\eta_{k'k})^2 \left| \begin{array}{c} \text{---} \square \text{---} \\ \text{---} \square \text{---} \\ \text{---} \square \text{---} \end{array} \right. \rangle. \quad (\text{C.2})$$

C.2 Commutative condition

The commutativity of the plaquette operators that act on the neighboring plaquettes in the GDW means $[B_{p_1}^{\text{DW}}, B_{p_2}^{\text{DW}}] = 0$. Here, we compute the action of $B_{p_1}^{\text{DW}} B_{p_2}^{\text{DW}}$ on a basis state:

$$\begin{aligned} & B_{p_1}^{\text{DW}} B_{p_2}^{\text{DW}} \left| \begin{array}{c} \text{---} \square \text{---} \\ \text{---} \square \text{---} \\ \text{---} \square \text{---} \end{array} \right. \rangle = \sum_{i_1, i_2 \in A_1, j_1, j_2 \in A_2} v_{i_1} v_{i_2} v_{j_1} v_{j_2} (\eta_{i_1 j_1} \eta_{i_2 j_2})^2 \left| \begin{array}{c} \text{---} \square \text{---} \\ \text{---} \square \text{---} \\ \text{---} \square \text{---} \end{array} \right. \rangle \\ & = \sum_{i_1, i_2, k_2, k_3 \in A_1} \sum_{j_1, j_2, l_2, l_3 \in A_2} \frac{v_{k_3} v_{l_3}}{v_{k_1} v_{l_1}} (\eta_{i_1 j_1} \eta_{i_2 j_2})^2 \left| \begin{array}{c} \text{---} \square \text{---} \\ \text{---} \square \text{---} \\ \text{---} \square \text{---} \end{array} \right. \rangle \\ & = \sum_{i_1, i_2, k_2, k_3, k'_2 \in A_1} \sum_{j_1, j_2, l_2, l_3, l'_2 \in A_2} \frac{v_{k_3} v_{l_3}}{v_{k_1} v_{l_1}} (\eta_{i_1 j_1} \eta_{i_2 j_2})^2 G_{i_1 k_1 k'_2}^{k_3^* k_2 l_2^*} G_{l_3 j_2 l'_2}^{l_1^* j_1 l_2} v_{l_2} v_{l'_2} v_{k_2} v_{k'_2} \left| \begin{array}{c} \text{---} \square \text{---} \\ \text{---} \square \text{---} \\ \text{---} \square \text{---} \end{array} \right. \rangle. \end{aligned}$$

To derive the commutativity condition for the plaquette operators, it is not necessary to fuse the entire loop. Instead, we focus on the shared edge between the two plaquettes and fuse only the relevant part of the string loop with it. Then, we compute the action of

$B_{p_2}^{\text{DW}} B_{p_1}^{\text{DW}}$ and using Pachner moves to transform the state into the same basis:

$$B_{p_2}^{\text{DW}} B_{p_1}^{\text{DW}} \left| \begin{array}{c} \text{---} \square \text{---} \\ \text{---} \square \text{---} \\ \text{---} \square \text{---} \end{array} \right\rangle = \sum_{i_1, i_2, k'_2, k_3 \in A_1} \sum_{j_1, j_2, l'_2, l_3 \in A_2} \frac{v_{k_3} v_{l_3}}{v_{k_1} v_{l_1}} (\eta_{i_1 j_1} \eta_{i_2 j_2})^2 \left| \begin{array}{c} \text{---} \square \text{---} \\ \text{---} \square \text{---} \\ \text{---} \square \text{---} \end{array} \right\rangle.$$

Then, the coefficients before the same basis states should match, leading to the formula below:

$$\sum_{\substack{k_2, k'_2 \in A_1 \\ l_2, l'_2 \in A_2}} \sum_{\substack{\eta_{i_1 j_1}, \eta_{i_2 j_2}, \eta_{k_1 l_1}, \\ \eta_{k_2 l_2}, \eta_{k_3 l_3} \neq 0}} G_{i_1 k_1 k'_2}^{k_3 k_2 i_2^*} G_{l_3 j_2 l'_2}^{l_1 j_1 l_2} v_{l_2} v_{l'_2} v_{k_2} v_{k'_2} f_{k_2^* k_3 i_2} f_{k_1^* i_1^* k_2} g_{l_2^* j_1 l_1} g_{l_3^* l_2 j_2^*} \\ = \sum_{\substack{k_2 \in A_1 \\ l_2 \in A_1}} \sum_{\substack{\eta_{i_1 j_1}, \eta_{i_2 j_2}, \eta_{k_1 l_1}, \\ \eta_{k_2 l_2}, \eta_{k_3 l_3} \neq 0}} f_{k_2^* i_1^* k_3} f_{k_1^* k_2 i_2} g_{l_2^* l_1 j_2^*} g_{l_3^* j_1 l_2}. \quad (\text{C.3})$$

The formula above can be represented graphically as:

$$\mathcal{T} \left(\left| \begin{array}{c} \text{---} \square \text{---} \\ \text{---} \square \text{---} \\ \text{---} \square \text{---} \end{array} \right\rangle \right) = \Delta[\eta_{i_1 j_1} \eta_{i_2 j_2} \eta_{k_1 l_1} \eta_{k_3 l_3}] \left| \begin{array}{c} \text{---} \square \text{---} \\ \text{---} \square \text{---} \\ \text{---} \square \text{---} \end{array} \right\rangle.$$

D Excitations in the GDW

D.1 Measuring operator at the GDW

In the derivation, we use the topological invariance of the Pachner moves.

$$\begin{aligned}
 \Pi_M \left| \begin{array}{c} \rho_1 \quad M_0 \quad \rho_2 \\ | \quad | \quad | \\ p \\ | \quad | \quad | \\ \rho_1 \quad M' \quad \rho_2 \end{array} \right\rangle &= \mathcal{T} \left(\left| \begin{array}{c} \rho_1 \quad M_0 \quad \rho_2 \\ | \quad | \quad | \\ M \\ | \quad | \quad | \\ \rho_1 \quad M' \quad \rho_2 \end{array} \right\rangle \xrightarrow{(3.19)} \left| \begin{array}{c} \rho_1 \quad M_0 \quad \rho_2 \\ | \quad | \quad | \\ M \\ | \quad | \quad | \\ \rho_1 \quad M' \quad \rho_2 \end{array} \right\rangle \right. \\
 &\xrightarrow{(4.1)} \left| \begin{array}{c} \rho_1 \quad M_0 \quad \rho_2 \\ | \quad | \quad | \\ M \\ | \quad | \quad | \\ \rho_1 \quad M' \quad \rho_2 \end{array} \right\rangle \xrightarrow{(4.1)} \left| \begin{array}{c} \rho_1 \quad M_0 \quad \rho_2 \\ | \quad | \quad | \\ M \\ | \quad | \quad | \\ \rho_1 \quad M' \quad \rho_2 \end{array} \right\rangle \\
 &\xrightarrow{(3.13)} \left| \begin{array}{c} \rho_1 \quad M_0 \quad \rho_2 \\ | \quad | \quad | \\ P_M \\ | \quad | \quad | \\ P_{M'} \\ | \quad | \quad | \\ \rho_1 \quad M' \quad \rho_2 \end{array} \right\rangle \xrightarrow{(3.5)} \delta_{M,M'} \left| \begin{array}{c} \rho_1 \quad M_0 \quad \rho_2 \\ | \quad | \quad | \\ p \\ | \quad | \quad | \\ \rho_1 \quad M \quad \rho_2 \end{array} \right\rangle \left. \right) \quad (D.1)
 \end{aligned}$$

D.2 Proof of $[B_p^{\text{DW}_6}, W_{E_1, E_2}^{e-m}] = 0$

First, we compute the action of $B_p^{\text{DW}_6} W_{E_1, E_2}^{e-m}$ on a basis state of a ground state:

$$B_p^{\text{DW}_6} W_{E_1, E_2}^{e-m} \left| \begin{array}{c} a_1 \quad b_1 \\ | \quad | \\ E_1 \quad i_1 \quad M_0 \quad j_1 \quad E_2 \\ | \quad | \quad | \quad | \\ p \\ | \quad | \quad | \quad | \\ i_3 \quad i_2 \quad M_0 \quad j_2 \quad j_3 \\ | \quad | \quad | \quad | \\ a_2 \quad b_2 \end{array} \right\rangle = B_p^{\text{DW}_6} \left([z_1^e]_{\psi \bar{i}_1 \psi i_1} [z_2^m]_{N_1 \bar{j}_1 N_1 j_1} \left| \begin{array}{c} a_1 \quad b_1 \\ | \quad | \\ \psi \quad \bar{i}_1 \quad \psi \quad M_0 \quad j_1 \\ | \quad | \quad | \quad | \\ \bar{j}_1 \quad N_1 \\ | \quad | \\ i_1 \quad i_2 \quad j_2 \quad j_3 \\ | \quad | \quad | \quad | \\ i_3 \quad a_2 \quad b_2 \end{array} \right\rangle \right), \quad (D.2)$$

where we use z_1^J and z_2^J to denote the half-braiding tensors of the \mathcal{C}_1 -model and the \mathcal{C}_2 -model, respectively, i.e., the $\mathcal{R}ep(\mathbb{Z}_2)$ -model and the $\mathcal{V}ec(\mathbb{Z}_2)$ in the e - m exchanging case of the toric code. According to the fusion rules of $\mathcal{R}ep(\mathbb{Z}_2)$ ($\mathcal{V}ec(\mathbb{Z}_2)$), fusing with the nontrivial object ψ (N_1) is equivalent to flipping the spin. We denote $\bar{1} = \psi, \bar{\psi} = 1$ and $\bar{N}_0 = N_1, \bar{N}_1 = N_0$. Thus, it is convenient to label the result of $i_1 \times \psi$ ($j_1 \times N_1$) to be \bar{i}_1

(\bar{j}_1). Then plugging $B_p^{\text{DW}_6} = \frac{B_p^{1N_0} + B_p^{\psi N_1}}{2}$ into Eq. (D.2), the R.H.S. becomes:

$$\begin{aligned}
\text{R.H.S.} &= B_p^{\text{DW}_6} \left([z_1^e]_{\psi i_1 \psi i_1} [z_2^m]_{N_1 \bar{j}_1 N_1 j_1} \left| \begin{array}{c} \bar{a}_1 \quad \bar{b}_1 \\ \psi \text{---} \bar{i}_1 \text{---} \square \text{---} \bar{j}_1 \\ i_1 \quad M_0 \quad j_1 \text{---} N_1 \\ i_3 \text{---} i_2 \quad j_2 \\ a_2 \text{---} \square \text{---} b_2 \end{array} \right. \right) \\
&= \frac{1}{2} [z_1^e]_{\psi i_1 \psi i_1} [z_2^m]_{N_1 \bar{j}_1 N_1 j_1} \left(\begin{array}{c} \bar{a}_1 \quad \bar{b}_1 \\ \psi \text{---} \bar{i}_1 \text{---} \square \text{---} \bar{j}_1 \\ i_1 \quad M_0 \quad j_1 \text{---} N_1 \\ i_3 \text{---} i_2 \quad j_2 \\ a_2 \text{---} \square \text{---} b_2 \end{array} + \begin{array}{c} a_1 \quad b_1 \\ \psi \text{---} i_1 \text{---} \square \text{---} j_1 \\ \bar{i}_1 \quad M_0 \quad \bar{j}_1 \text{---} N_1 \\ i_3 \text{---} \bar{i}_2 \quad \bar{j}_2 \\ \bar{a}_2 \text{---} \square \text{---} \bar{b}_2 \end{array} \right). \tag{D.3}
\end{aligned}$$

Second, we compute the action of $W_{E_1, E_2}^{e-m} B_p^{\text{DW}_6}$:

$$\begin{aligned}
W_{E_1, E_2}^{e-m} B_p^{\text{DW}_6} \left| \begin{array}{c} a_1 \quad b_1 \\ E_1 \text{---} i_1 \text{---} \square \text{---} j_1 \text{---} E_2 \\ p \\ i_3 \text{---} i_2 \quad M_0 \quad j_2 \\ a_2 \text{---} \square \text{---} b_2 \end{array} \right\rangle &= \frac{1}{2} W_{E_1, E_2}^{e-m} \left(\left| \begin{array}{c} a_1 \quad b_1 \\ i_1 \quad M_0 \quad j_1 \\ i_3 \text{---} i_2 \quad j_2 \\ a_2 \text{---} \square \text{---} b_2 \end{array} \right\rangle + \left| \begin{array}{c} \bar{a}_1 \quad \bar{b}_1 \\ i_1 \quad M_0 \quad \bar{j}_1 \\ i_3 \text{---} i_2 \quad \bar{j}_2 \\ a_2 \text{---} \square \text{---} b_2 \end{array} \right\rangle \right) \\
&= \frac{1}{2} \left([z_1^e]_{\psi i_1 \psi i_1} [z_2^m]_{N_1 \bar{j}_1 N_1 j_1} \left| \begin{array}{c} \bar{a}_1 \quad \bar{b}_1 \\ \psi \text{---} \bar{i}_1 \text{---} \square \text{---} \bar{j}_1 \\ i_1 \quad M_0 \quad j_1 \text{---} N_1 \\ i_3 \text{---} i_2 \quad j_2 \\ a_2 \text{---} \square \text{---} b_2 \end{array} \right. \right) + [z_1^e]_{\psi i_1 \psi i_1} [z_2^m]_{N_1 j_1 N_1 \bar{j}_1} \left| \begin{array}{c} a_1 \quad b_1 \\ \psi \text{---} i_1 \text{---} \square \text{---} j_1 \\ \bar{i}_1 \quad M_0 \quad \bar{j}_1 \text{---} N_1 \\ i_3 \text{---} \bar{i}_2 \quad \bar{j}_2 \\ \bar{a}_2 \text{---} \square \text{---} \bar{b}_2 \end{array} \right. \right). \tag{D.4}
\end{aligned}$$

According to the results of the half-braiding tensors given in B.1 and B.2, we find the ratio $[z_1^e]_{\psi i_1 \psi i_1} / [z_1^e]_{\psi \bar{i}_1 \psi i_1} = 1$ for any $i_1 \in \{1, \psi\}$ and $[z_2^m]_{N_1 j_1 N_1 \bar{j}_1} / [z_2^m]_{N_1 \bar{j}_1 N_1 j_1} = 1$ for any $j_1 \in \{N_0, N_1\}$, we have $[z_1^e]_{\psi i_1 \psi i_1} [z_2^m]_{N_1 j_1 N_1 \bar{j}_1} = [z_1^e]_{\psi \bar{i}_1 \psi i_1} [z_2^m]_{N_1 \bar{j}_1 N_1 j_1}$, which implies that Eq. (D.3) and (D.4) yield the same result. Consequently, the DW plaquette operator $B_p^{\text{DW}_6}$ commutes with the DW-crossing operator W_{E_1, E_2}^{e-m} , making it the shortest ribbon operator across the GDW.

From the computation above, we find that the shortest ribbon operator across the e - m exchanging GDW in the toric code should satisfy the two conditions: (1) the tail of the anyon created in the $\mathcal{R}ep(\mathbb{Z}_2)$ -model and the tail of the anyon created in the $\mathcal{V}ec(\mathbb{Z}_2)$ -model should simultaneously be 1 and N_0 , or ψ and N_1 ; (2) the ratio $[z_1^{J_1}]_{q\bar{i}q\bar{i}} / [z_1^J]_{q\bar{i}q\bar{i}}$ for any $i \in \{1, \psi\}$ and $[z_2^{J_2}]_{q\bar{j}q\bar{j}} / [z_2^{J'}]_{q\bar{j}q\bar{j}}$ for any $j \in \{N_0, N_1\}$ should be the same, so the GDW-crossing operator $W_{E_1, E_2}^{J_1 - J_2}$ can commute with the plaquette operator B_p^{DW} . Taking

these two conditions into account, there are only four types of GDW cross-over operator, which are W_{E_1, E_2}^{1-1} , W_{E_1, E_2}^{e-m} , W_{E_1, E_2}^{m-e} , $W_{E_1, E_2}^{\epsilon-\epsilon}$.

E Solutions for joining functions η in specific cases

E.1 Case 1: $A_1 = A_2$

Consider the case where two algebras A_1 and A_2 are the same, i.e., $L_{A_1} = L_{A_2} \subset L_1$ and $f_{abc} = g_{abc}$. For simplicity, we denote both A_1 and A_2 by A . Then, there is a solution for (3.21) and (3.23) that $f_{ijk} = g_{ijk} = \delta_{ijk}$, and the joining function $\eta_{ij} = \sqrt{D_A^{-1}}\delta_{ij}$. Here, δ_{ij} is the Kronecker delta and $D_A = \sum_{i \in A} d_i^2$ is the total quantum dimension of the input algebra A in the GDW.

We can check by putting the solution back in Eqs. (3.21) and (3.23). The commutative condition (3.21) would become:

$$\sum_{k'_2 \in A} G_{k'_1 i_1 k'_2}^{k_3 i_2 k_2^*} G_{j_2^* l_3^* l'_2}^{j_1 l_1 l_2^*} d_{k_2} d_{k'_2} = \delta_{k'_2 i_1 k_3} \delta_{k'_1 k'_2 i_2}. \quad (\text{E.1})$$

We can replace the $\sum_{k'_2 \in A}$ by $k'_2 \in \mathcal{C}_1$ in the LHS because the terms newly added are zero indeed. More precisely, when $k'_2 \notin L_A$, then $\delta_{k'_2 i_1 k_3} = 0$ for $\forall i_1, k_3 \in L_A$ because the multiplication of the algebra A is closed, and accordingly the 6j-symbol $G_{k'_1 i_1 k'_2}^{k_3 i_2 k_2^*}$ would vanish. After rewriting the summation, Eq. (E.1) becomes exactly the orthogonality condition of 6j-symbols (A.7) in the \mathcal{C}_1 -model.

Moreover, the projective condition (3.23) becomes:

$$\sum_{i, j \in A} \delta_{ijk^*} \frac{d_i d_j}{d_k} D_A^{-1} = 1, \quad (\text{E.2})$$

According to the fusion rules, the equation $\sum_{i \in L_1} \delta_{ijk^*} d_i = d_j d_k$ with $i, j, k \in L_1$ holds as a one-dimensional representation. Since also the multiplication $f_{ijk} = \delta_{ijk}$ is closed, we have $\sum_{i \in A} \delta_{ijk^*} d_i = d_j d_k$ for $\forall i, j, k \in L_A$. Substitute this condition into the LHS of Eq. E.2, then $(\sum_{j \in A} d_j)^2 d_k D_A^{-1} = d_k$, which apparently holds.

In particular, if $\mathcal{C}_1 = \mathcal{C}_2$ and $A_1 = A_2 = \text{Ob}(\mathcal{C}_1)$, then $\eta_{ij} = \sqrt{D^{-1}}\delta_{ij}$ corresponds to the trivial GDW, which does not differ from the bulk region.

E.2 Case 2: $A_1 = 1$ or $A_2 = 1$

Another case is that one of the input algebras in the GDW is trivial, say $A_2 = 1$ (the following analyses are the same for $A_1 = 1$). Then the only non-vanishing multiplication g_{ijk} is $g_{111} = 1$. Then the joining function in this case is $\eta_{ij} = \sqrt{d_A^{-1}}\delta_{j1}$, with δ_{j1} the Kronecker delta, and $d_{A_1} = \sum_{i \in A_1} d_i$.

Also, plug the solution into Eq. (3.21) and (3.23) to have a check. The commutative condition (3.21) would become:

$$\sum_{k_2 \in A_1} f_{k_2^* k_3 i_2} f_{k_1^* i_1 k_2} \sum_{k'_2 \in A_1} G_{i_1 k_1 k'_2}^{k_3^* k_2 i_2^*} v_{k_2} v_{k'_2} = \sum_{k'_2 \in A_1} f_{k'_2 i_1 k_3} f_{k_1^* k'_2 i_2}, \quad (\text{E.3})$$

which can be expressed diagrammatically,

$$\mathcal{T} \left| \begin{array}{c} \xrightarrow{k_3} \bullet \xrightarrow{k_2} \bullet \xrightarrow{k_1} \\ \uparrow i_2 \\ \downarrow i_1 \end{array} \right\rangle = \left| \begin{array}{c} \xrightarrow{k_3} \bullet \xrightarrow{k'_2} \bullet \xrightarrow{k_1} \\ \uparrow i_1 \\ \downarrow i_2 \end{array} \right\rangle. \quad (\text{E.4})$$

This equation (E.4) is exactly the associativity condition of the input Frobenius algebras that characterize the GBs of the LW model with the input UFC \mathcal{C}_1 [8]. In this case, the GDW joins one GB characterized by A_1 of the \mathcal{C}_1 -model and a smooth GB with $A_2 = 1$ of the \mathcal{C}_2 -model. The gluing process is trivial.

The projective condition (3.23) would become:

$$\sum_{i', j' \in A_1} \delta_{i' j' k'^*} \frac{v_{i'} v_{j'}}{v_{k'}} f_{i' j' k'^*} f_{k' i' j'^*} d_{A_1} = 1, \quad (\text{E.5})$$

This equation coincides with the strong condition of the Frobenius algebras [8].

F Minimal solutions of $A_1 \overset{\eta}{-} A_2$ -bimodules

F.1 $A_1 \overset{\eta}{-} A_2$ -bimodules for the LW \mathbb{Z}_2 model

F.1.1 $\mathcal{C}_1 = \mathcal{C}_2 = \text{Rep}(\mathbb{Z}_2)$

When $A_1 = A_2 = 1$ with $f_{111} = g_{111} = 1$, and $\eta_{11} = 1$, then solving Eq. (3.5) will produce the two irreducible $A_1 \overset{\eta}{-} A_2$ -bimodules, which are characterized by minimal solutions of P -tensors as below:

- $M_0 = 1$

$$P_{111}^{11} = 1 \quad (\text{F.1})$$

- $M_1 = \psi$

$$P_{\psi\psi\psi}^{11} = 1 \quad (\text{F.2})$$

For $A_1 = 1 \oplus \psi$ with $f_{abc} = \delta_{abc}$, and $A_2 = 1$ with $g_{111} = 1$, $\eta_{ab} = \frac{1}{\sqrt{2}} \delta_{a \in \{1, \psi\}} \delta_{b, 1}$, there are two irreducible $A_1 \overset{\eta}{-} A_2$ -bimodules:

- $M_0 = 1 \oplus \psi$

$$P_{111}^{11} = 1 \quad P_{\psi\psi\psi}^{11} = 1 \quad P_{\psi\psi 1}^{1\psi} = 1 \quad P_{11\psi}^{1\psi} = 1 \quad (\text{F.3})$$

- $M_1 = 1 \oplus \psi$

$$P_{111}^{11} = 1 \quad P_{\psi\psi\psi}^{11} = 1 \quad P_{\psi\psi 1}^{1\psi} = i \quad P_{11\psi}^{1\psi} = -i \quad (\text{F.4})$$

For $A_1 = 1$ with $f_{111} = 1$, and $A_2 = 1 \oplus \psi$ with $g_{abc} = \delta_{abc}$, $\eta_{ab} = \frac{1}{\sqrt{2}} \delta_{a, 1} \delta_{b \in \{1, \psi\}}$, there are two irreducible $A_1 \overset{\eta}{-} A_2$ -bimodules:

- $M_0 = 1 \oplus \psi$

$$P_{111}^{11} = 1 \quad P_{\psi\psi\psi}^{11} = 1 \quad P_{1\psi\psi}^{1\psi} = 1 \quad P_{\psi 11}^{1\psi} = 1 \quad (\text{F.5})$$

- $M_1 = 1 \oplus \psi$

$$P_{111}^{11} = 1 \quad P_{\psi\psi\psi}^{11} = 1 \quad P_{1\psi\psi}^{1\psi} = i \quad P_{\psi 11}^{1\psi} = -i \quad (\text{F.6})$$

For $A_1 = A_2 = 1 \oplus \psi$ with $f_{abc} = g_{abc} = \delta_{abc}$, and $\eta_{ab} = \frac{1}{2}\delta_{a \in \{1, \psi\}}\delta_{b \in \{1, \psi\}}$, there are also two irreducible $A_1 \overset{\eta}{-} A_2$ -bimodules:

- $M_0 = 1 \oplus \psi$

$$\begin{aligned} P_{111}^{11} &= 1 & P_{\psi\psi\psi}^{11} &= 1 & P_{1\psi\psi}^{1\psi} &= 1 & P_{\psi 11}^{1\psi} &= 1 \\ P_{\psi\psi 1}^{\psi 1} &= 1 & P_{11\psi}^{\psi 1} &= 1 & P_{1\psi 1}^{\psi\psi} &= 1 & P_{\psi 1\psi}^{\psi\psi} &= 1 \end{aligned} \quad (\text{F.7})$$

- $M_1 = 1 \oplus \psi$

$$\begin{aligned} P_{111}^{11} &= 1 & P_{\psi\psi\psi}^{11} &= 1 & P_{1\psi\psi}^{1\psi} &= i & P_{\psi 11}^{1\psi} &= -i \\ P_{\psi\psi 1}^{\psi 1} &= i & P_{11\psi}^{\psi 1} &= -i & P_{1\psi 1}^{\psi\psi} &= -1 & P_{\psi 1\psi}^{\psi\psi} &= -1 \end{aligned} \quad (\text{F.8})$$

In this case, the $A_1 \overset{\eta}{-} A_2$ -bimodules are the same as the conventional A_1 - A_2 -bimodules.

When $\eta_{ab} = \frac{1}{\sqrt{d_{A_1} d_{A_2}}}\delta_{a \in A_1}\delta_{b \in A_2}$, the solutions above for $A_1 \overset{\eta}{-} A_2$ -bimodules are the same to the conventional A_1 - A_2 -bimodules.

For $A_1 = A_2 = 1 \oplus \psi$ with $f_{abc} = g_{abc} = \delta_{abc}$, and $\eta_{ab} = \frac{1}{\sqrt{d_A}}\delta_{ab}, \forall a, b \in A$, there are four irreducible $A_1 \overset{\eta}{-} A_2$ -bimodules for the \mathbb{Z}_2 LW model listed as follows:

- $M_0 = 1$

$$P_{111}^{11} = 1 \quad P_{1\psi 1}^{\psi\psi} = 1 \quad (\text{F.9})$$

- $M_1 = \psi$

$$P_{\psi\psi\psi}^{11} = 1 \quad P_{\psi 1\psi}^{\psi\psi} = 1 \quad (\text{F.10})$$

- $M_2 = 1$

$$P_{111}^{11} = 1 \quad P_{1\psi 1}^{\psi\psi} = -1 \quad (\text{F.11})$$

- $M_3 = \psi$

$$P_{\psi\psi\psi}^{11} = 1 \quad P_{\psi 1\psi}^{\psi\psi} = -1 \quad (\text{F.12})$$

F.1.2 $\mathcal{C}_1 = \mathcal{R}ep(\mathbb{Z}_2), \mathcal{C}_2 = \mathcal{V}ec(\mathbb{Z}_2)$

When $A_1 = 1$ with $f_{111} = 1$, and $A_2 = N_0 \oplus N_1$ with $g_{N_i N_j N_k} = \delta_{N_i N_j N_k}$ are both Frobenius algebras. Then the multiplication after basis transformation is

$$\begin{aligned} g_{111}^{N_0 N_0 N_0} &= g_{1\psi\psi}^{N_0 N_0 N_0} = g_{\psi\psi 1}^{N_0 N_0 N_0} = g_{\psi 1\psi}^{N_0 N_0 N_0} = 1, \\ g_{111}^{N_0 N_1 N_1} &= g_{1\psi\psi}^{N_0 N_1 N_1} = 1, \quad g_{\psi\psi 1}^{N_0 N_1 N_1} = g_{\psi 1\psi}^{N_0 N_1 N_1} = -1, \end{aligned} \quad (\text{F.13})$$

with cyclic symmetry. When $\eta_{1N_0} = \eta_{1N_1} = \frac{1}{\sqrt{2}}$, the two $A_1 \overset{\eta}{-} A_2$ -bimodules are the same as Eq. (F.1) and (F.2). Nevertheless, when $A_1 = 1 \oplus \psi$ with $f_{abc} = \delta_{abc}$, and $\eta_{1N_0} = \eta_{1N_1} = \eta_{\psi N_0} = \eta_{\psi N_1} = \frac{1}{2}$, there are two $A_1 \overset{\eta}{-} A_2$ -bimodules which are the same as Eq. (F.3) and Eq. (F.4).

When $A = 1$ with $f_{111} = 1$, and $A_2 = N_0$ with $g_{N_0 N_0 N_0} = 1$ are both Frobenius algebras. Then the multiplication after basis transformation is

$$g_{111}^{N_0 N_0 N_0} = g_{1\psi\psi}^{N_0 N_0 N_0} = g_{\psi\psi 1}^{N_0 N_0 N_0} = g_{\psi 1\psi}^{N_0 N_0 N_0} = 1. \quad (\text{F.14})$$

Then the two $A_1 \overset{\eta}{-} A_2$ -bimodules are the same as Eq. (F.5) and (F.6).

When $A_1 = 1 \oplus \psi$ with $f_{abc} = \delta_{abc}$, and $A_2 = N_0$ with $g_{N_0 N_0 N_0} = 1$ are both Frobenius algebras. The two $A_1 - A_2$ -bimodules are the same as Eq. (F.7) and (F.8).

When $A_1 = 1 \oplus \psi$ with $f_{abc} = \delta_{abc}$, $A_2 = N_0 \oplus N_1$ with $g_{N_i N_j N_k} = \delta_{N_i N_j N_k}$. Then A_2 has different multiplication after basis transformation as shown below:

$$\begin{aligned} \tilde{g}_{111}^{N_0 N_0 N_0} &= \tilde{g}_{1\psi\psi}^{N_0 N_0 N_0} = \tilde{g}_{\psi 1\psi}^{N_0 N_0 N_0} = \tilde{g}_{\psi\psi 1}^{N_0 N_0 N_0} = 1 \\ \tilde{g}_{111}^{N_0 N_1 N_1} &= \tilde{g}_{1\psi\psi}^{N_0 N_1 N_1} = 1, \quad \tilde{g}_{\psi\psi 1}^{N_0 N_1 N_1} = i, \quad \tilde{g}_{\psi 1\psi}^{N_0 N_1 N_1} = -i. \end{aligned} \quad (\text{F.15})$$

The gluing function is $\eta_{1N_0} = \eta_{\psi N_1} = \frac{1}{\sqrt{2}}$. Then there are four irreducible $A_1 - A_2$ -bimodules:

- $M_0 = 1 \oplus \psi$

$$\begin{aligned} P_{111}^{11} &= 1 & P_{\psi\psi\psi}^{11} &= 1 & P_{1\psi\psi}^{1\psi} &= -i & P_{\psi 11}^{1\psi} &= i \\ P_{\psi\psi 1}^{\psi 1} &= 1 & P_{11\psi}^{\psi 1} &= 1 & P_{1\psi 1}^{\psi\psi} &= 1 & P_{\psi 1\psi}^{\psi\psi} &= -1 \end{aligned} \quad (\text{F.16})$$

- $M_1 = 1 \oplus \psi$

$$\begin{aligned} P_{111}^{11} &= 1 & P_{\psi\psi\psi}^{11} &= 1 & P_{1\psi\psi}^{1\psi} &= i & P_{\psi 11}^{1\psi} &= -i \\ P_{\psi\psi 1}^{\psi 1} &= -1 & P_{11\psi}^{\psi 1} &= -1 & P_{1\psi 1}^{\psi\psi} &= 1 & P_{\psi 1\psi}^{\psi\psi} &= -1 \end{aligned} \quad (\text{F.17})$$

- $M_2 = 1 \oplus \psi$

$$\begin{aligned} P_{111}^{11} &= 1 & P_{\psi\psi\psi}^{11} &= 1 & P_{1\psi\psi}^{1\psi} &= -i & P_{\psi 11}^{1\psi} &= i \\ P_{\psi\psi 1}^{\psi 1} &= -1 & P_{11\psi}^{\psi 1} &= -1 & P_{1\psi 1}^{\psi\psi} &= -1 & P_{\psi 1\psi}^{\psi\psi} &= 1 \end{aligned} \quad (\text{F.18})$$

- $M_3 = 1 \oplus \psi$

$$\begin{aligned} P_{111}^{11} &= 1 & P_{\psi\psi\psi}^{11} &= 1 & P_{1\psi\psi}^{1\psi} &= i & P_{\psi 11}^{1\psi} &= -i \\ P_{\psi\psi 1}^{\psi 1} &= 1 & P_{11\psi}^{\psi 1} &= 1 & P_{1\psi 1}^{\psi\psi} &= -1 & P_{\psi 1\psi}^{\psi\psi} &= 1 \end{aligned} \quad (\text{F.19})$$

F.2 $A_1 - A_2$ -bimodules for the Ising LW model

When $A = 1$ and $\eta_{11} = 1$, there are three irreducible A -bimodules:

- $M_0 = 1$

$$P_{111}^{11} = 1 \quad (\text{F.20})$$

- $M_1 = \psi$

$$P_{\psi\psi\psi}^{11} = 1 \quad (\text{F.21})$$

- $M_2 = \sigma$

$$P_{\sigma\sigma\sigma}^{11} = 1 \quad (\text{F.22})$$

When $A = 1 \oplus \psi$, and $\eta_{ab} = \delta_{a \in \{1, \psi\}} \delta_{b \in \{1, \psi\}}$ is separable, there are also three irreducible $A_1 - A_2$ -bimodules.

- $M_0 = 1 \oplus \psi$

$$\begin{aligned} P_{111}^{11} &= 1 & P_{\psi\psi\psi}^{11} &= 1 & P_{1\psi\psi}^{1\psi} &= 1 & P_{\psi 11}^{1\psi} &= 1 \\ P_{\psi\psi 1}^{\psi 1} &= 1 & P_{11\psi}^{\psi 1} &= 1 & P_{1\psi 1}^{\psi\psi} &= 1 & P_{\psi 1\psi}^{\psi\psi} &= 1 \end{aligned} \quad (\text{F.23})$$

- $M_1 = 1 \oplus \psi$

$$\begin{aligned} P_{111}^{11} &= 1 & P_{\psi\psi\psi}^{11} &= 1 & P_{1\psi\psi}^{1\psi} &= -1 & P_{\psi 11}^{1\psi} &= -1 \\ P_{\psi\psi 1}^{\psi 1} &= 1 & P_{11\psi}^{\psi 1} &= 1 & P_{1\psi 1}^{\psi\psi} &= -1 & P_{\psi 1\psi}^{\psi\psi} &= -1 \end{aligned} \quad (\text{F.24})$$

- $M_2 = \sigma_1 \oplus \sigma_2$

$$\begin{aligned}
P_{\sigma_1\sigma_1\sigma_1}^{11} &= \frac{1}{4} & P_{\sigma_1\sigma_2\sigma_1}^{11} &= \frac{1}{4} & P_{\sigma_2\sigma_1\sigma_2}^{11} &= \frac{1}{4} & P_{\sigma_2\sigma_2\sigma_2}^{11} &= \frac{1}{4} \\
P_{\sigma_1\sigma_1\sigma_1}^{1\psi} &= \frac{1}{4} & P_{\sigma_1\sigma_2\sigma_1}^{1\psi} &= \frac{1}{4} & P_{\sigma_2\sigma_1\sigma_2}^{1\psi} &= -\frac{1}{4} & P_{\sigma_2\sigma_2\sigma_2}^{1\psi} &= -\frac{1}{4} \\
P_{\sigma_1\sigma_1\sigma_2}^{\psi 1} &= \frac{1}{4} & P_{\sigma_2\sigma_1\sigma_1}^{\psi 1} &= \frac{1}{4} & P_{\sigma_2\sigma_2\sigma_1}^{\psi 1} &= \frac{1}{4} & P_{\sigma_1\sigma_2\sigma_2}^{\psi 1} &= \frac{1}{4} \\
P_{\sigma_1\sigma_1\sigma_2}^{\psi\psi} &= -\frac{1}{4} & P_{\sigma_1\sigma_2\sigma_2}^{\psi\psi} &= -\frac{1}{4} & P_{\sigma_2\sigma_1\sigma_1}^{\psi\psi} &= \frac{1}{4} & P_{\sigma_2\sigma_2\sigma_1}^{\psi\psi} &= \frac{1}{4}
\end{aligned} \tag{F.25}$$

When $A = 1 \oplus \psi$, and $\eta_{ab} = \delta_{ab}, \forall a, b \in A$, there are six irreducible $A_1 \overset{\eta}{-} A_2$ -bimodules for $A = 1 \oplus \psi$:

- $M_0 = 1$

$$P_{111}^{11} = 1 \quad P_{1\psi 1}^{\psi\psi} = 1 \tag{F.26}$$

- $M_1 = \psi$

$$P_{\psi\psi\psi}^{11} = 1 \quad P_{\psi 1\psi}^{\psi\psi} = 1 \tag{F.27}$$

- $M_2 = 1$

$$P_{111}^{11} = 1 \quad P_{1\psi 1}^{\psi\psi} = -1 \tag{F.28}$$

- $M_3 = \psi$

$$P_{\psi\psi\psi}^{11} = 1 \quad P_{\psi 1\psi}^{\psi\psi} = -1 \tag{F.29}$$

- $M_4 = \sigma$

$$P_{\sigma\sigma\sigma}^{11} = 1 \quad P_{\sigma\sigma\sigma}^{\psi\psi} = i \tag{F.30}$$

- $M_5 = \sigma$

$$P_{\sigma\sigma\sigma}^{11} = 1 \quad P_{\sigma\sigma\sigma}^{\psi\psi} = -i \tag{F.31}$$

References

- [1] A. Kapustin and N. Saulina, *Topological boundary conditions in abelian chern–simons theory*, *Nuclear Physics B* **845** (2011) 393.
- [2] J. Fuchs, C. Schweigert and A. Valentino, *Bicategories for boundary conditions and for surface defects in 3-d tft*, *Communications in Mathematical Physics* **321** (2013) 543.
- [3] T. Lan, J.C. Wang and X.-G. Wen, *Gapped domain walls, gapped boundaries, and topological degeneracy*, *Physical review letters* **114** (2015) 076402.
- [4] A. Kitaev and L. Kong, *Models for Gapped Boundaries and Domain Walls*, *Communications in Mathematical Physics* **313** (2012) .
- [5] Z. Jia, D. Kaszlikowski and S. Tan, *Boundary and domain wall theories of 2d generalized quantum double model*, *Journal of High Energy Physics* **2023** (2023) 1.
- [6] Y. Zhao, S. Huang, H. Wang, Y. Hu and Y. Wan, *Characteristic properties of a composite system of topological phases separated by gapped domain walls via an exactly solvable hamiltonian model*, *SciPost Physics Core* **6** (2023) 076.
- [7] J. Christian, D. Green, P. Huston and D. Penneys, *A lattice model for condensation in levin-wen systems*, *Journal of High Energy Physics* **2023** (2023) 1.

- [8] Y. Hu, Z.-X. Luo, R. Pankovich, Y. Wan and Y.-S. Wu, *Boundary hamiltonian theory for gapped topological phases on an open surface*, *Journal of High Energy Physics* **2018** (2018) 1.
- [9] S. Beigi, P.W. Shor and D. Whalen, *The quantum double model with boundary: condensations and symmetries*, *Communications in mathematical physics* **306** (2011) 663.
- [10] I. Cong and Z. Wang, *Topological quantum computation with gapped boundaries and boundary defects*, *Topological Phases of Matter and Quantum Computation* (2017) .
- [11] I. Cong, M. Cheng and Z. Wang, *Universal quantum computation with gapped boundaries*, *Physical Review Letters* **119** (2017) 170504.
- [12] F.A. Bais and J.K. Slingerland, *Condensate-induced transitions between topologically ordered phases*, *Physical Review B* **79** (2009) .
- [13] F.A. Bais, J.K. Slingerland and S.M. Haaker, *Theory of topological edges and domain walls*, *Physical Review Letters* **102** (2009) .
- [14] L. Kong, *Anyon condensation and tensor categories*, *Nuclear Physics B* **886** (2014) .
- [15] T. Neupert, H. He, C. Von Keyserlingk, G. Sierra and B.A. Bernevig, *Boson condensation in topologically ordered quantum liquids*, *Physical Review B* **93** (2016) 115103.
- [16] Y. Hu, Z. Huang, L.-Y. Hung and Y. Wan, *Anyon condensation: coherent states, symmetry enriched topological phases, goldstone theorem, and dynamical rearrangement of symmetry*, *Journal of High Energy Physics* **2022** (2022) 1.
- [17] M.S. Kesselring, J.C. Magdalena de la Fuente, F. Thomsen, J. Eisert, S.D. Bartlett and B.J. Brown, *Anyon condensation and the color code*, *PRX Quantum* **5** (2024) 010342.
- [18] Y. Zhao, H. Wang, Y. Hu and Y. Wan, *Symmetry fractionalized (irrationalized) fusion rules and two domain-wall verlinde formulae*, *Journal of High Energy Physics* **2024** (2024) 1.
- [19] Y. Zhao and Y. Wan, *Nonabelian anyon condensation in 2+ 1d topological orders: A string-net model realization*, *arXiv preprint arXiv:2409.05852* (2024) .
- [20] H. Bombín, *Topological order with a twist: Ising anyons from an abelian model*, *Physical review letters* **105** (2010) 030403.
- [21] O. Buerschaper, M. Christandl, L. Kong and M. Aguado, *Electric–magnetic duality of lattice systems with topological order*, *Nuclear Physics B* **876** (2013) 619.
- [22] H. Wang, Y. Li, Y. Hu and Y. Wan, *Electric-magnetic duality in the quantum double models of topological orders with gapped boundaries*, *Journal of High Energy Physics* **2020** (2020) 1.
- [23] Y. Hu and Y. Wan, *Electric-magnetic duality in twisted quantum double model of topological orders*, *Journal of High Energy Physics* **2020** (2020) 1.
- [24] P. Huston, F. Burnell, C. Jones and D. Penneys, *Composing topological domain walls and anyon mobility*, *SciPost Physics* **15** (2023) 076.
- [25] Y. Hu, N. Geer and Y.-S. Wu, *Full dyon excitation spectrum in extended levin-wen models*, *Physical Review B* **97** (2018) 195154.
- [26] L.Y. Hung and Y. Wan, *Generalized ADE classification of topological boundaries and anyon condensation*, *Journal of High Energy Physics* (2015) .
- [27] J. Kock, *Frobenius Algebras and 2-D Topological Quantum Field Theories*, London Mathematical Society Student Texts, Cambridge University Press (2003).

- [28] H. Wang, Y. Hu and Y. Wan, *Extend the levin-wen model to two-dimensional topological orders with gapped boundary junctions*, *Journal of High Energy Physics* **2022** (2022) 1.
- [29] M.A. Levin and X.-G. Wen, *String-net condensation: A physical mechanism for topological phases*, *Physical Review B* **71** (2005) 045110.
- [30] Y. Zhao and Y. Wan, *Noninvertible gauge symmetry in $(2+1)$ d topological orders: A string-net model realization*, *arXiv preprint arXiv:2408.02664* (2024) .